

NEURAL NETWORKS AS INTERACTING PARTICLE SYSTEMS: ASYMPTOTIC CONVEXITY OF THE LOSS LANDSCAPE AND UNIVERSAL SCALING OF THE APPROXIMATION ERROR

GRANT M. ROTSKOFF AND ERIC VANDEN-EIJNDEN

ABSTRACT. Neural networks, a central tool in machine learning, have demonstrated remarkable, high fidelity performance on image recognition and classification tasks. These successes evince an ability to accurately represent high dimensional functions, potentially of great use in computational and applied mathematics. That said, there are few rigorous results about the representation error and trainability of neural networks, as well as how they scale with the network size. Here we characterize both the error and scaling by reinterpreting the standard optimization algorithm used in machine learning applications, stochastic gradient descent, as the evolution of a particle system with interactions governed by a potential related to the objective or “loss” function used to train the network. We show that, when the number n of parameters is large, the empirical distribution of the particles descends on a convex landscape towards a minimizer at a rate independent of n . We establish a Law of Large Numbers and a Central Limit Theorem for the empirical distribution, which together show that the approximation error of the network universally scales as $o(n^{-1})$. Remarkably, these properties do not depend on the dimensionality of the domain of the function that we seek to represent. Our analysis also quantifies the scale and nature of the noise introduced by stochastic gradient descent and provides guidelines for the step size and batch size to use when training a neural network. We illustrate our findings on examples in which we train neural network to learn the energy function of the continuous 3-spin model on the sphere. The approximation error scales as our analysis predicts in as high a dimension as $d = 25$.

CONTENTS

1. Motivation and main results	2
1.1. Problem set-up	3
1.2. Functional formulation	4
1.3. Universal Representation Theorem	4
1.4. Parameters as particles with loss function as interaction potential	5
1.5. Finite training set and stochastic gradient descent	6
1.6. Universal scaling error of neural networks	6
1.7. Style and organization	6
2. Interacting particles with adaptive fractional charges for training	7
2.1. Empirical distribution and Dean’s equations	7
2.2. Limit behavior and fluctuations scaling	8
2.3. Law of Large Numbers (LLN)	12
2.4. Central Limit Theorem (CLT)	13
3. Finite training set and stochastic gradient descent (SGD)	14
3.1. Limiting stochastic differential equation (SDE)	15
3.2. Dean’s equation for particles with correlated noise	16
3.3. Limit behavior and fluctuations scaling in SGD	17
3.4. Law of Large Number and Central Limit Theorem for SGD	18
4. Illustrative example: 3-spin model on the high-dimensional sphere	20
4.1. Learning with Gaussian kernels	20

We thank Weinan E for discussions about the approximation error of neural networks and Sylvia Serfaty for her insights about interacting particle systems.

4.2. Learning with single layer networks with sigmoid nonlinearity	21
5. Concluding remarks	23
References	24

1. MOTIVATION AND MAIN RESULTS

While classification problems continue to be an active area research, extraordinary progress has been made on both speech and image recognition, problems that appeared intractable only a decade ago [1]. By harvesting the power of neural networks while simultaneously benefiting from advances in computational hardware, complex tasks such as automatic language translation are now routinely performed by computers with a high degree of reliability. The underlying explanation for these significant advances seems to be related to the expressive power of neural networks, and their ability to represent high dimensional functions with accuracy.

These successes open exciting possibilities in applied and computational mathematics that are only beginning to be explored [2–8]. Any numerical calculation that uses a given function begins with a finite-dimensional representation of that function. Because standard approximations, e.g., Galerkin truncations or finite element decompositions, suffer from the curse of dimensionality, it is nearly impossible to scale such methods to large dimensions d . Fundamentally, these representations are linear combinations of basis functions. The issue arises because the dimensionality of the representation is equal to that of the truncation. Neural networks, on the other hand, are highly nonlinear in their adjusting parameters. As a result, their effective dimensionality is much higher than the number of their parameters, which may explain their better capabilities observed in practice to approximate functions even when d is large. Characterizing this observation with analysis is non-trivial though, precisely because the representation of a function by a neural network is nonlinear in its parameters. This renders many of the standard tools of numerical analysis useless, since they are in large part based on linear algebra.

The significant achievements of machine learning have inspired many efforts to provide theoretical justification to a vast and growing body of empirical knowledge. At the core of our understanding of neural networks are the “Universal Approximation Theorems” that specify the conditions under which a neural network can represent a target function with arbitrary accuracy [9–11]. These results do not, however, indicate how the network parameters should be determined to achieve maximal accuracy when their number is fixed [12]. Additionally, these theorems do not provide guidance on how the error scales with the number of parameters. Several recent papers have focused on the analysis of the shape and properties of the objective or “loss” function landscape [13–15]. These studies have mainly focused on the fine features of this landscape, trying to understand how non-convex it is and making analogies with glassy landscapes. Additionally, some analysis has been performed in cases where the number of parameters vastly exceeds the amount of training data, a setting that guarantees convexity and dramatically simplifies the landscape. Further studies have examined the dynamics of the parameters on the loss landscape to understand the properties of optimization procedures based on stochastic gradient descent.

In this paper, similar to what was recently proposed in [16], we adopt a different perspective which enables powerful tools for a more formal analysis. We view the parameters in the network as particles and the loss function as a potential that dictates the interaction between them. Correspondingly, training the network is thought of as the evolution of the particles in this interaction potential. We also consider the empirical distribution of the n interacting particles / parameters and analyze the properties of this distribution when the number n is large using standard limit theorems [17–20]. This viewpoint allows us to bypass many of the difficulties that arise with approaches that attempt to study the dynamics of the individual particles. For example, we rederive the Universal Approximation Theorem as a corollary to the Law of Large Number (LLN) for the

empirical distribution of the particles. We also establish that the loss landscape is asymptotically convex for large n in the space of the empirical distribution of the particles, and assert that convergence towards equilibrium of this distribution occurs on a time scale that is independent of n to leading order— similar results were also obtained in [16]. Finally, we prove a Central Limit Theorem for the empirical distribution, and thereby conclude that the approximation error of the function representation by a neural network is universal and scales as $O(n^{-1})$ as $n \rightarrow \infty$. Let us briefly elaborate on these statements next, starting with a precise formulation of the problem.

1.1. Problem set-up. Given a function $f : \Omega \rightarrow \mathbb{R}$ defined on $\Omega \subseteq \mathbb{R}^d$, consider its approximation by

$$(1.1) \quad f_n(\mathbf{x}) = \frac{1}{n} \sum_{i=1}^n c_i \varphi(\mathbf{x}, \mathbf{y}_i)$$

where $n \in \mathbb{N}$, $(c_i, \mathbf{y}_i) \in \mathbb{R} \times D$ with $D \subset \mathbb{R}^N$ are parameters to be learned for $i = 1, \dots, n$, and $\varphi : \Omega \times D \rightarrow \mathbb{R}$ is some kernel whose properties will be specified below and about which we make

Assumption 1.1. *The kernel $\varphi : \Omega \times D \rightarrow \mathbb{R}$ is smooth in both its arguments, \mathbf{x} and \mathbf{y} , and bounded $\max_{\mathbf{x} \in \Omega, \mathbf{y} \in D} \varphi(\mathbf{x}, \mathbf{y}) < \infty$.*

Many models used in machine learning can be cast in the form (1.1):

- **Radial basis function network.** In this case $D \equiv \Omega$ and $\varphi(\mathbf{x}, \mathbf{y}) \equiv \phi(\mathbf{x} - \mathbf{y})$ where ϕ is some kernel, for example that of a radial function such as

$$\phi(\mathbf{x}) = \exp\left(-\frac{1}{2}\kappa|\mathbf{x}|^2\right)$$

where $\kappa > 0$ is a fixed constant.

- **Single layer neural networks.** In this case, $D \equiv \mathbb{R}^{d+1}$ and $\varphi(\mathbf{x}, \mathbf{y}) = \varphi(\mathbf{x}, \mathbf{a}, b)$ with $\mathbf{a} \in \mathbb{R}^d$, $b \in \mathbb{R}$, and

$$\varphi(\mathbf{x}, \mathbf{a}, b) = h(\mathbf{a} \cdot \mathbf{x} + b)$$

where $h : \mathbb{R} \rightarrow \mathbb{R}$ is e.g. a sigmoid function $h(z) = 1/(1 + e^{-z})$.

- **Deep neural networks.** These are essentially iterated versions of single layer neural networks.

In view of the growing range of applications of these methods, it is natural to ask:

- (1) How good can the approximation (1.1) be if we optimize $\{(c_i, \mathbf{y}_i)\}_{i=1}^n$?
- (2) Can we guarantee the convergence of the commonly used optimization algorithms?

To answer the first question, we need to introduce a distance, or loss function, between f and f_n . A natural candidate often used in practice is

$$(1.2) \quad \ell(f, f_n) = \frac{1}{2} \int_{\Omega} |f(\mathbf{x}) - f_n(\mathbf{x})|^2 d\mu(\mathbf{x})$$

where μ is some measure on Ω with a positive density and such that $\mu(\Omega) < \infty$ (for example the Lebesgue measure, $d\mu(\mathbf{x}) = d\mathbf{x}$, if Ω is compact). This also offers a way to address the second question, since we can view $\ell(f, f_n)$ as an objective function for $\{(c_i, \mathbf{y}_i)\}_{i=1}^n$:

$$(1.3) \quad \ell(f, f_n) = C_f - \frac{1}{n} \sum_{i=1}^n c_i F(\mathbf{y}_i) + \frac{1}{2n^2} \sum_{i,j=1}^n c_i c_j K(\mathbf{y}_i, \mathbf{y}_j)$$

where $C_f = \frac{1}{2} \int_{\Omega} |f(\mathbf{x})|^2 d\mu(\mathbf{x})$ and we defined

$$(1.4) \quad F(\mathbf{y}) = \int_{\Omega} f(\mathbf{x}) \varphi(\mathbf{x}, \mathbf{y}) d\mu(\mathbf{x}), \quad K(\mathbf{y}, \mathbf{z}) = \int_{\Omega} \varphi(\mathbf{x}, \mathbf{y}) \varphi(\mathbf{x}, \mathbf{z}) d\mu(\mathbf{x}) \equiv K(\mathbf{z}, \mathbf{y}).$$

Trying to minimize (1.3) over $\{(c_i, \mathbf{y}_i)\}_{i=1}^n$ leads to difficulties, however, since this is potentially (and presumably) a non-convex optimization problem, which will typically have local minimizers. As a result determining the distance (1.2) at the minimum (and its scaling with n , say) is

also nontrivial. To bypass these difficulties we will study the problem in terms of its empirical distribution.

1.2. Functional formulation. Assume that the set $\{(c_i, \mathbf{y}_i)\}_{i=1}^n$ is such that

$$(1.5) \quad f_n \rightarrow \tilde{f} = \int_D \varphi(\cdot, \mathbf{y}) G(\mathbf{y}) d\mathbf{y} \quad \text{as } n \rightarrow \infty$$

for some signed density G on D . If $\varphi(\mathbf{x}, \cdot)$ is smooth, a sufficient condition is that the empirical measure

$$(1.6) \quad d\gamma_n(\mathbf{y}) = \frac{1}{n} \sum_{i=1}^n c_i \delta_{\mathbf{y}_i}(d\mathbf{y}) \equiv \frac{1}{n} \sum_{i=1}^n c_i \delta(\mathbf{y} - \mathbf{y}_i) d\mathbf{y}$$

converges weakly to $G(\mathbf{y}) d\mathbf{y}$ as $n \rightarrow \infty$. Clearly, this can be achieved e.g. by drawing the \mathbf{y}_i 's independently from some probability density function $\bar{\rho}(\mathbf{y})$ such that $\bar{\rho}(\mathbf{y}) > 0$ for all $\mathbf{y} \in D$ and $\int_D \bar{\rho}(\mathbf{y}) d\mathbf{y} = 1$, and setting $c_i = G(\mathbf{y}_i) / \bar{\rho}(\mathbf{y}_i)$: we then have $d\gamma_n(\mathbf{y}) \rightarrow G(\mathbf{y}) d\mathbf{y}$ as $n \rightarrow \infty$ by the Law of Large Numbers, with an error scaling as $O(n^{-1/2})$ by the Central Limit Theorem—we will see that this scaling can be improved upon. In this limit, (1.3) converges to an objective function for G :

$$(1.7) \quad \ell(f, \tilde{f}) = C_f - \int_D F(\mathbf{y}) G(\mathbf{y}) d\mathbf{y} + \frac{1}{2} \int_{D \times D} K(\mathbf{y}, \mathbf{z}) G(\mathbf{y}) G(\mathbf{z}) d\mathbf{y} d\mathbf{z}$$

Unlike (1.3), this objective function is quadratic in G . This means that minimizing (1.7) over G rather than (1.3) over $\{(c_i, \mathbf{y}_i)\}_{i=1}^n$ is conceptually simpler than a direct minimization.

1.3. Universal Representation Theorem. To formalize these ideas, it is useful to view φ as a map from $L^2(D)$ to $L^2(\Omega, \mu)$ and introduce also its adjoint $\varphi^\dagger : L^2(\Omega, \mu) \rightarrow L^2(D)$. These operators are defined for any suitable $G \in L^2(D)$ and $g \in L^2(\Omega, \mu)$ respectively as

$$(1.8) \quad \varphi G = \int_D \varphi(\cdot, \mathbf{y}) G(\mathbf{y}) d\mathbf{y}, \quad \varphi^\dagger g = \int_\Omega g(\mathbf{x}) \varphi(\mathbf{x}, \cdot) d\mu(\mathbf{x})$$

We can then write the loss function in (1.2) evaluated on $f_n = \varphi G$ as

$$(1.9) \quad \ell(f, \varphi G) = \frac{1}{2} \|f - \varphi G\|_{L^2(\Omega, \mu)}^2$$

and the question becomes whether there exists a minimizer G^* of this objective function with $\varphi G^* = f$. Note that any such minimizer is also a solution to the Euler-Lagrange equation for both (1.9) and (1.7):

$$(1.10) \quad F = KG \quad \text{explicitly:} \quad F(\mathbf{y}) = \int_D K(\mathbf{y}, \mathbf{y}') G(\mathbf{y}') d\mathbf{y}'$$

where F and K are given explicitly in (1.4). We can also express these operators as $F = \varphi^\dagger f$ and $K = \varphi^\dagger \varphi$: viewed as an operator mapping $L^2(D)$ into itself, K is symmetric and nonnegative.

This question of existence of solutions to (1.15) is within the realm of Fredholm theory of integral equations of the first kind [21]. For neural networks, it is natural to make:

Assumption 1.2. *The operator φ is bounded, i.e. $\exists c > 0 : \|\varphi G\|_{L^2(\Omega, \mu)} \leq c \|G\|_{L^2(D)} \forall G \in L^2(D)$, and square integrable:*

$$(1.11) \quad \int_D \int_\Omega |\varphi(\mathbf{x}, \mathbf{y})|^2 d\mu(\mathbf{x}) d\mathbf{y} < \infty$$

Indeed this assumption holds for the kernels used in machine learning, and it guarantees that both φ and φ^\dagger are compact operators whose domains are $L^2(D)$ and $L^2(\Omega, \mu)$, respectively. Under Assumption 1.2, it is well known that (1.9) admits at least one minimizer (and (1.15) at least one solution) if and only if $f \in \text{ran } \varphi \cup \text{ran } \varphi^\dagger$ (where 'ran' denotes the range of the operator), which is a dense subspace of $L^2(\Omega, \mu)$. This solution/minimizer may not be unique, since we can add to it any element of null φ , which is not necessarily trivial. In the present context, this is no real

issue, however, since we only care that φG gives f for any solution G of (1.15). This suggests that we make:

Assumption 1.3 (Discriminating Kernel). *The null space of the adjoint $\varphi^\dagger : L^2(\Omega, \mu) \rightarrow L^2(D)$ is trivial, i.e.*

$$(1.12) \quad \varphi^\dagger g = 0 \text{ a.e. in } D \Rightarrow g = 0 \text{ a.e. in } \Omega$$

We can then summarize the discussion above into:

Theorem 1.4 (Universal Representation Theorem). *Under Assumptions 1.2 and 1.3, given any $f \in L^2(\Omega, \mu)$ and $\epsilon > 0$, there exists $f^* \in \text{ran } \varphi \cup \text{ran } \bar{\varphi}$ which is such that*

$$(1.13) \quad \|f - f^*\|_{L^2(\Omega, \mu)} \leq \epsilon$$

and admits the representation

$$(1.14) \quad \varphi G^* = f^* \text{ a.e. in } \Omega$$

where G^* solves

$$(1.15) \quad F^* = K G^* \quad \text{with } F^* = \bar{\varphi} f^*$$

The function f^* can also be realized as

$$(1.16) \quad f^* = \lim_{n \rightarrow \infty} \frac{1}{n} \sum_{i=1}^n c_j \varphi(\cdot, \mathbf{y}_j)$$

for some choice of $\{\mathbf{y}_i, c_i\}_{i \in \mathbb{N}}$.

Proof. By Assumption 1.2, (1.15) admits at least one solution G^* if $F^* = \bar{\varphi} f^*$ and $f^* \in \text{ran } \varphi \cup \text{ran } \bar{\varphi}$, and since this subspace is dense in $L^2(\Omega, \mu)$, (1.13) can be satisfied. By writing (1.15) as

$$(1.17) \quad 0 = \bar{\varphi}(f^* - \varphi G^*)$$

we see that (1.14) follows by Assumption 1.3. To show that there is a choice of $\{\mathbf{y}_i, c_i\}_{i \in \mathbb{N}}$ such that (1.16) holds pick, for example, the \mathbf{y}_i independently from some probability density function $\bar{\rho}(\mathbf{y})$ such that $\bar{\rho}(\mathbf{y}) > 0$ for all $\mathbf{y} \in D$ and $\int_D \bar{\rho}(\mathbf{y}) d\mathbf{y} = 1$, and set $c_i = G^*(\mathbf{y}_i) / \bar{\rho}(\mathbf{y}_i)$. (1.16) then follows by the Law of Large Numbers. \square

The Universal Representation Theorem only gives F^* , not f , but this suffices in our case since we cannot manipulate (1.15) directly, but rather need to go back to the representation (1.6). This introduces errors due to the finiteness of n which, even if they decrease as $n \rightarrow \infty$, will remain larger than those induced by replacing f by f^* if we pick ϵ small enough. In other words, we can bound $\ell(f, f_n) \leq \ell(f, f^*) + \ell(f^*, f_n)$ and make $\ell(f, f^*)$ smaller than $\ell(f^*, f_n)$. For this reason, in what follows we will not distinguish f from f^* . What remains to be shown, however, is that the Universal Representation Theorem can be approximately realized in practice via dynamic training of the parameters in (1.1) (recall that we have no direct access to G^*). In addition we seek to assess quantitatively the rate of convergence in time toward this approximation and the error due to the finiteness of n . This aim will be achieved by treating the parameters $\{\mathbf{y}_i, c_i\}_{i=1}^n$ as a set of interacting particles.

1.4. Parameters as particles with loss function as interaction potential. As we will show, it is useful to view the set $\{\mathbf{y}_i, c_i\}_{i=1}^n$ as particles (with \mathbf{y}_i viewed as a particle position and c_i as its charge), and use (1.3) as an interaction potential between them. In this interpretation, we can perform the training by making these parameters evolve by gradient descent (GD) in this potential, or stochastic gradient descent (SGD)—the method of choice used in machine learning to train neural networks. If we denote these time-dependent parameters as $\{\mathbf{Y}_i(t), C_i(t)\}_{i=1}^n$ with $t \geq 0$, we will study the way

$$(1.18) \quad f_n(t, \mathbf{x}) = \frac{1}{n} \sum_{i=1}^n C_i(t) \varphi(\mathbf{x}, \mathbf{Y}_i(t))$$

evolves in time, as well as the behavior of this function for large n . In particular, we will establish a Law of Large Numbers (LLN) for $f_n(t)$ as well as a Central Limit Theorem (CLT), and thereby assess the error and trainability of neural networks representations.

1.5. Finite training set and stochastic gradient descent. For most choices of the kernel φ commonly encountered in machine learning it is not possible to calculate (1.2) and (1.4) exactly. Rather we will have to approximate these integrals using a training set, i.e. a set of points $\{\mathbf{x}_p\}_{p=1}^P$ distributed according to μ , possibly independent, and over which f is known. We will then approximate $\ell(f, f_n)$ by

$$(1.19) \quad \ell_P(f, f_n) = \frac{1}{P} \sum_{p=1}^P |f(\mathbf{x}_p) - f_n(\mathbf{x}_p)|^2$$

and F and/or K by

$$(1.20) \quad F_P(\mathbf{y}) = \frac{1}{P} \sum_{i=1}^P f(\mathbf{x}_p) \varphi(\mathbf{x}_p, \mathbf{y}), \quad K_P(\mathbf{y}, \mathbf{z}) = \frac{1}{P} \sum_{p=1}^P \varphi(\mathbf{x}_p, \mathbf{y}) \varphi(\mathbf{x}_p, \mathbf{z}).$$

These approximations are precisely what SGD relies upon to calculate the gradient of the interaction potential / loss function, and we will assess the errors they introduce.

We will focus on situations in which we can redraw the training set as often as we need (e.g. at every step during the learning process). In this case, in the limit as the updating time step Δt used in SGD tends to zero, SGD becomes asymptotically equivalent to an SDE whose drift terms coincide with those on GD but with small multiplicative noise terms added.

1.6. Universal scaling error of neural networks. The main results we obtain can be summarized as follows: the function (1.18) evolves with GD on a convex landscape (quadratic at leading order in n) and is such that

$$(1.21) \quad f_n(t) \sim f + o(n^{-1}) \quad \text{for large } t$$

with a convergence rate in time that is independent of n to leading order as $n \rightarrow \infty$. This scaling also holds for SGD if we choose the size P of the batch used in (1.20) such that as $P = O(n^2)$. If we set $P = O(n^{2\alpha})$ with $\alpha \in (0, 1]$, then we loose accuracy and (1.21) is replaced by

$$(1.22) \quad f_n(t) \sim f + o(n^{-\alpha}) \quad \text{for large } t.$$

If we set $P = O(n^{2\alpha})$ with $\alpha > 1$, there is no gain and we get (1.21) back. These results are stated in Proposition 2.3 in the context of GD and in Proposition 3.2 in the context of SGD.

1.7. Style and organization. As is apparent from the discussion above, our approach has strong ties with the statistical mechanics of systems of many interacting particles. This is an active area of research in which rigorous results have been obtained recently, primarily in the context of Coulomb or Riesz interaction potentials. These potentials lead to kernels that are not compact operators. The situation we consider here is therefore different, and simpler in some technical ways. The main additional issues we face are that (i) our kernels are degenerate, i.e. φ is not injective in general, and (ii) the charges are not fixed, but rather are being considered as evolving particles themselves.

Despite these difficulties, we believe that providing rigorous proof to each of our statements can be achieved using the mathematical apparati developed in the context of interacting particle systems. We will not undertake such an endeavor here, however. Rather we will adopt a semi-rigorous presentation and rely on formal asymptotic arguments to derive our results. This has the advantage of making the developments easier to follow.

The remainder of this paper is organized as follows:

In Sec. 2 we study a model system of interacting particles undergoing gradient descent on the network loss function—this dynamics is close to the stochastic gradient descent used in machine

learning to train networks but more readily amenable to analysis. The equations for the empirical distribution of the particles are derived in Sec. 2.1. In Sec. 2.2 we study the limiting behavior of the empirical distribution and analyze the scaling of the fluctuations around this limit. The equations derived this way are then used in Sec. 2.3 to establish a Law of Large Numbers and in Sec. 2.4 a Central Limit Theorem. These results have direct implications in terms of the approximation error of the function representation by the neural network and its scaling with the number of particles. They also have implications for the dynamics of the training.

We then study stochastic gradient descent in Sec. 3, where we revisit all our results in this practical context: In Sec. 3.1 we derive the stochastic differential equation (SDE) to which SGD is asymptotically equivalent for small time steps and large batch size. The SDEs we obtain have multiplicative noise terms added on the top of the drift terms in the GD equations studied in Sec. 2. The limiting behavior of the empirical distribution and the scaling of the fluctuations around it are then analyzed in Sec. 3.4 where we rederive a LLN and a CLT in the context of SGD, and discuss again their implications in terms of approximation error and trainability.

These results are illustrated in Sec. 4, where we use a spherical p -spin model with $p = 3$ as test case of a complex function to represent with a neural network. We show that the network accurately approximates this function in up to $d = 25$ dimensions, with a scaling of the error consistent with the results established in Secs. 2 and 3. These results are obtained using both a radial basis function network, and a single-layer network using sigmoid functions.

Some concluding remarks are made in Sec. 5.

2. INTERACTING PARTICLES WITH ADAPTIVE FRACTIONAL CHARGES FOR TRAINING

Here we define an idealized set of dynamical equations for $\{\mathbf{Y}_i(t), C_i(t)\}_{i=1}^n$ that can be used to train the network by updating its parameters dynamically, and we analyze these equations as $n \rightarrow \infty$ and $t \rightarrow \infty$. Specifically, we assume that $\{\mathbf{Y}_i(t), C_i(t)\}_{i=1}^n$ satisfy the following system of ordinary differential equations (ODEs):

$$(2.1) \quad \begin{cases} \dot{\mathbf{Y}}_i = C_i \nabla F(\mathbf{Y}_i) - \frac{1}{n} \sum_{j=1}^n C_i C_j \nabla K(\mathbf{Y}_i, \mathbf{Y}_j), \\ \dot{C}_i = F(\mathbf{Y}_i) - \frac{1}{n} \sum_{j=1}^n C_j K(\mathbf{Y}_i, \mathbf{Y}_j) \end{cases}$$

for $i = 1, \dots, n$. As we show in Sec. 3, (2.1) share some properties with the stochastic gradient descent, though in the case of SGD a multiplicative noise term persists in the equations. The ODEs in (2.1) are the gradient descent flow on the energy:

$$(2.2) \quad E(c_1, \mathbf{y}_1, \dots, c_n, \mathbf{y}_n) = - \sum_{i=1}^n c_i F(\mathbf{y}_i) + \frac{1}{2n} \sum_{i,j=1}^n c_i c_j K(\mathbf{y}_i, \mathbf{y}_j)$$

This energy is simply the loss function in (1.3) rescaled by n .

We will consider (2.1) with initial conditions such that every pair in $\{\mathbf{Y}_i(0), C_i(0)\}_{i=1}^n$ is drawn independently from some probability density function $\rho_{\text{in}}(\mathbf{y}, c)$. We denote the measure for the infinite set $\{(\mathbf{Y}_i(0), C_i(0))\}_{i \in \mathbb{N}}$ constructed this way by \mathbb{P}_{in} . Initial conditions of this type are frequently used in practice.

2.1. Empirical distribution and Dean's equations. To proceed, we consider the empirical distribution

$$(2.3) \quad \rho_n(t, \mathbf{y}, c) = \frac{1}{n} \sum_{i=1}^n \delta(c - C_i(t)) \delta(\mathbf{y} - \mathbf{Y}_i(t))$$

in terms of which we can express (1.18) as

$$(2.4) \quad f_n(t, \mathbf{x}) = \frac{1}{n} \sum_{i=1}^n C_i(t) \varphi(\mathbf{x}, \mathbf{Y}_i(t)) = \int_{D \times R} c \varphi(\mathbf{x}, \mathbf{y}) \rho_n(t, \mathbf{y}, c) d\mathbf{y} dc$$

The empirical distribution (2.3) is useful to work with because it satisfies

$$(2.5) \quad \begin{aligned} \partial_t \rho_n = \nabla \cdot & \left(-c \nabla F \rho_n + \int_{D \times \mathbb{R}} c c' \nabla K(\mathbf{y}, \mathbf{y}') \rho'_n \rho_n d\mathbf{y}' dc' \right) \\ & + \partial_c \left(-F \rho_n + \int_{D \times \mathbb{R}} c' K(\mathbf{y}, \mathbf{y}') \rho'_n \rho_n d\mathbf{y}' dc' \right) \end{aligned}$$

where we used the shorthand notation $\rho_n = \rho_n(t, \mathbf{y}, c)$.

When there is noise, (2.5) is often referred to as Dean's equation [22]. It should be viewed as a formal identity which is useful to analyze the properties of ρ_n as $n \rightarrow \infty$, as we will do in Secs. 2.2, 2.3 and 2.4.

Derivation of Dean's equation (2.5). Let us take the time derivative of (2.3). By the chain rule:

$$(2.6) \quad \begin{aligned} \partial_t \rho_n(t, \mathbf{y}, c) = & -\frac{1}{n} \sum_{i=1}^n \delta(c - C_i) \nabla \delta(\mathbf{y} - \mathbf{Y}_i) \cdot \dot{\mathbf{Y}}_i \\ & - \frac{1}{n} \sum_{i=1}^n \partial_c \delta(c - C_i) \delta(\mathbf{y} - \mathbf{Y}_i) \dot{C}_i \end{aligned}$$

Pulling the derivatives in front of the sums and using (2.1) we can write this equation as

$$(2.7) \quad \begin{aligned} \partial_t \rho_n(t, \mathbf{y}, c) = & -\nabla \cdot \left(\frac{1}{n} \sum_{i=1}^n \delta(c - C_i) \delta(\mathbf{y} - \mathbf{Y}_i(t)) \left(c \nabla F(\mathbf{y}) - \frac{1}{n} \sum_{j=1}^n c C_j \nabla K(\mathbf{y}, \mathbf{Y}_j) \right) \right) \\ & - \partial_c \left(\frac{1}{n} \sum_{i=1}^n \delta(c - C_i) \delta(\mathbf{y} - \mathbf{Y}_i) \left(F(\mathbf{y}) - \frac{1}{n} \sum_{j=1}^n C_j K(\mathbf{y}, \mathbf{Y}_j) \right) \right) \end{aligned}$$

where we used the Dirac delta to replace \mathbf{Y}_i by \mathbf{y} and C_i by c . We can now use the definition of ρ_n to replace $\frac{1}{n} \sum_{i=1}^n \delta(c - C_i(t)) \delta(\mathbf{y} - \mathbf{Y}_i(t))$ by $\rho_n(t, \mathbf{y}, c)$. In addition, if we use

$$(2.8) \quad \begin{aligned} \frac{1}{n} \sum_{j=1}^n c C_j \nabla K(\mathbf{y}, \mathbf{Y}_j) &= \frac{1}{n} \sum_{j=1}^n \int_{D \times \mathbb{R}} c c' \nabla K(\mathbf{y}, \mathbf{y}') \delta(c' - C_j) \delta(\mathbf{y}' - \mathbf{Y}_j) d\mathbf{y}' dc' \\ &= \int_{D \times \mathbb{R}} c c' \nabla K(\mathbf{y}, \mathbf{y}') \rho_n(t, c', \mathbf{y}') d\mathbf{y}' dc' \end{aligned}$$

and similarly for $\frac{1}{n} \sum_{j=1}^n C_j K(\mathbf{y}, \mathbf{Y}_j)$, we see that we can write the right hand side of (2.7) precisely as that in (2.5).

2.2. Limit behavior and fluctuations scaling. Let us now use Dean's equation (2.5) to derive equations for the limit of ρ_n as $n \rightarrow \infty$ and for the fluctuations around this limit. All limits will be understood in weak (or distributional) sense, which is what matters to us since at the end we care about $f_n(t)$, not $\rho_n(t)$ itself, and $f_n(t)$ is obtained by testing $\rho_n(t)$ against $c\varphi(\cdot, \mathbf{y})$, as in (2.4).

2.2.1. Zeroth order term—mean field limit. If we formally take the limit as $n \rightarrow \infty$ of (2.5), we deduce that $\rho_n(t) \rightarrow \rho_0(t)$, where $\rho_0(t)$ satisfies

$$(2.9) \quad \begin{aligned} \partial_t \rho_0 = \nabla \cdot & \left(-c \nabla F \rho_0 + \int_{D \times \mathbb{R}} c c' \nabla K(\mathbf{y}, \mathbf{y}') \rho'_0 \rho_0 d\mathbf{y}' dc' \right) \\ & + \partial_c \left(-F \rho_0 + \int_{D \times \mathbb{R}} c' K(\mathbf{y}, \mathbf{y}') \rho'_0 \rho_0 d\mathbf{y}' dc' \right). \end{aligned}$$

Here and below we use the prime as shorthand notation to indicate dependency in (\mathbf{y}', c') , i.e. $\rho'_0 = \rho_0(t, \mathbf{y}', c')$. Notice that (2.9) can be written as

$$(2.10) \quad \partial_t \rho_0 = \nabla \cdot \left(\rho_0 \nabla \frac{\delta \mathcal{E}_0}{\delta \rho_0} \right) + \partial_c \left(\rho_0 \partial_c \frac{\delta \mathcal{E}_0}{\delta \rho_0} \right)$$

where $\mathcal{E}_0[\rho_0]$ is given by:

$$(2.11) \quad \mathcal{E}_0[\rho_0] = - \int_{D \times \mathbb{R}} c F \rho_0 d\mathbf{y} dc + \frac{1}{2} \int_{(D \times \mathbb{R})^2} c c' K(\mathbf{y}, \mathbf{y}') \rho_0 \rho_0' d\mathbf{y} dc d\mathbf{y}' dc'$$

In (2.10) we can also write

$$(2.12) \quad \frac{\delta \mathcal{E}_0}{\delta \rho_0} = F_0(t) - F$$

where we defined

$$(2.13) \quad F_0(t, \mathbf{y}) = \int_{D \times \mathbb{R}} c' \nabla K(\mathbf{y}, \mathbf{y}') \rho_0(t, \mathbf{y}', c') d\mathbf{y}' dc'$$

Even though (2.9) is formally identical to (2.5), it has a different meaning since we can look for a smooth solution of it (that is, (2.9) no longer is an equation for a distribution): As a result of the initial conditions for (2.1), we know that \mathbb{P}_{in} -almost surely as $n \rightarrow \infty$, $\rho_n(0, \mathbf{y}, c) \rightarrow \rho_{\text{in}}(\mathbf{y}, c)$ by the Law of Large Numbers. However, to justify that $\rho_0(t)$, the solution of (2.9) for this initial condition, is indeed the weak limit of the empirical distribution $\rho_n(t)$ at later times, we will have to control the fluctuations of $\rho_n(t)$ around $\rho_0(t)$. We do this next and postpone the analysis of (2.9) until Sec. 2.3.

2.2.2. Fluctuations around the mean. Let us now consider the fluctuations of $\rho_n(t)$ around $\rho_0(t)$. The scale of these fluctuations change with time and to account for this effect, we define $\tilde{\rho}_\xi(t)$ via:

$$(2.14) \quad \rho_n = \rho_0 + n^{-\xi(t)} \tilde{\rho}_\xi(t),$$

where the exponent $\xi(t)$ will be allowed to depend on t as specified below. Explicitly, (2.14) means:

$$(2.15) \quad \tilde{\rho}_\xi(t)(t, \mathbf{y}, c) = n^{\xi(t)-1} \sum_{i=1}^n (\delta(\mathbf{y} - \mathbf{Y}_i(t)) \delta(c - C_i(t)) - \rho_0(t, \mathbf{y}, c))$$

By the Central Limit Theorem, choosing $\xi(0) = 1/2$ sets the right scale to look at the fluctuations around the initial conditions. Indeed, if we pick a test function $\chi : D \times \mathbb{R} \rightarrow \mathbb{R}$, the CLT tells us that under \mathbb{P}_{in}

$$(2.16) \quad \int_{D \times \mathbb{R}} \chi(\mathbf{y}, c) \tilde{\rho}_{\xi(0)}(0, \mathbf{y}, c) d\mathbf{y} dc = n^{-1/2} \sum_{i=1}^n \tilde{\chi}(\mathbf{Y}_i(0), C_i(0)) \rightarrow N(0, C_\chi) \quad \text{in law as } n \rightarrow \infty$$

where $N(0, C_\chi)$ denotes the Gaussian random variable with mean zero and variance C_χ , and we defined

$$(2.17) \quad \tilde{\chi}(\mathbf{y}, c) = \chi(\mathbf{y}, c) - \int_{D \times \mathbb{R}} \chi(\mathbf{y}, c) \rho_{\text{in}}(\mathbf{y}, c) d\mathbf{y} dc, \quad C_\chi = \int_{D \times \mathbb{R}} |\tilde{\chi}(\mathbf{y}, c)|^2 \rho_{\text{in}}(\mathbf{y}, c) d\mathbf{y} dc,$$

We can write (2.16) distributionally as

$$(2.18) \quad \tilde{\rho}_{\xi(0)}(0, \mathbf{y}, c) \rightarrow N(0, \rho_{\text{in}}(\mathbf{y}, c) \delta(\mathbf{y} - \mathbf{y}') \delta(c - c')) \quad \text{in law as } n \rightarrow \infty$$

To see what happens at later times, we derive an equation for $\tilde{\rho}_\xi(t)$ by subtracting (2.9) from (2.5) and using (2.14)

$$(2.19) \quad \begin{aligned} \partial_t \tilde{\rho}_\xi(t) = & \nabla \cdot \left(-c \nabla F \tilde{\rho}_\xi(t) + \int_{D \times \mathbb{R}} c c' \nabla K(\mathbf{y}, \mathbf{y}') (\tilde{\rho}'_{\xi(t)} \rho_0 + \rho_0' \tilde{\rho}_\xi(t) + n^{-\xi(t)} \tilde{\rho}'_{\xi(t)} \tilde{\rho}_\xi(t)) d\mathbf{y}' dc' \right) \\ & + \partial_c \left(-F \tilde{\rho}_\xi(t) + \int_{D \times \mathbb{R}} c' K(\mathbf{y}, \mathbf{y}') (\tilde{\rho}'_{\xi(t)} \rho_0 + \rho_0' \tilde{\rho}_\xi(t) + n^{-\xi(t)} \tilde{\rho}'_{\xi(t)} \tilde{\rho}_\xi(t)) d\mathbf{y}' dc' \right) \\ & + \dot{\xi}(t) \log n \tilde{\rho}_\xi(t) \end{aligned}$$

In order to take the limit as $n \rightarrow \infty$ of this equation, we need to consider carefully the behavior of the factors in (2.19) that contain n explicitly, that is, $n^{-\xi(t)} \tilde{\rho}_{\xi(t)} \tilde{\rho}'_{\xi(t)}$ and $\dot{\xi}(t) \log n \tilde{\rho}_{\xi(t)}$. Consider the latter first. If we set

$$(2.20) \quad \dot{\xi}(t) \log n = o(1)$$

the last term at the right hand side of (2.19) will be higher order. Note that (2.20) means that we can vary $\xi(t)$, but only slowly. For the factor $n^{-\xi(t)} \tilde{\rho}_{\xi(t)} \tilde{\rho}'_{\xi(t)}$, a direct calculation shows that, for any $p \in \mathbb{N}$ and $\xi \in \mathbb{R}$,

$$(2.21) \quad \mathbb{E}_{\text{in}} \left(n^{-\xi} \int_{(D \times \mathbb{R})^2} \chi(\mathbf{y}, c) \chi(\mathbf{y}', c') \tilde{\rho}_{\xi} \tilde{\rho}'_{\xi} d\mathbf{y} d\mathbf{c} d\mathbf{y}' d\mathbf{c}' \right)^p = O\left(n^{(\xi-1)p}\right)$$

where \mathbb{E}_{in} denotes expectation with respect to \mathbb{P}_{in} —for example, if $p = 1$, this expectation is $n^{(\xi-1)} C_{\chi}$ where C_{χ} is given in (2.17). (2.21) implies that \mathbb{P}_{in} -almost surely as $n \rightarrow \infty$, $n^{-\xi} \tilde{\rho}_n(0) \tilde{\rho}'_n(0) \rightarrow 0$ at $t = 0$ if $\xi < 1$. We can now argue that this statement also holds at times $t > 0$ if (2.20) holds. To this end we write (2.19) compactly as

$$(2.22) \quad \partial_t \tilde{\rho}_{\xi(t)} = L \tilde{\rho}_{\xi(t)} + R_{\xi(t)} + \dot{\xi}(t) \log n \tilde{\rho}_{\xi(t)}$$

where $L \tilde{\rho}_n$ contains the terms at the right hand side of (2.19) that are linear in $\tilde{\rho}_{\xi(t)}$, and $R_{\xi(t)}$ contains the terms involving $n^{-\xi(t)} \tilde{\rho}_{\xi(t)} \tilde{\rho}'_{\xi(t)}$. In order to control the $R_{\xi(t)}$ term, we can write an equation for $n^{-\xi(t)} \tilde{\rho}_{\xi(t)} \tilde{\rho}'_{\xi(t)}$: this equation will be of the form (2.22) with an additional linear term involving L' (same as L but acting on (\mathbf{y}', c')), the source term $R_{\xi(t)}$ replaced by one involving $n^{-2\xi(t)} \tilde{\rho}_{\xi(t)} \tilde{\rho}'_{\xi(t)} \tilde{\rho}''_{\xi(t)}$, and the last term in (2.22) replaced by $2\dot{\xi}(t) \log n \tilde{\rho}_{\xi(t)} \tilde{\rho}'_{\xi(t)}$: a calculation similar to the one that gives (2.21) indicates that at $t = 0$ this source term is higher order than the rest and goes to zero \mathbb{P}_{in} -almost surely as $n \rightarrow \infty$. The same is true for $2\dot{\xi}(t) \log n \tilde{\rho}_{\xi(t)} \tilde{\rho}'_{\xi(t)}$ if (2.20) holds. We can then derive equations for $n^{-2\chi(t)} \tilde{\rho}_{\xi(t)} \tilde{\rho}'_{\xi(t)} \tilde{\rho}''_{\xi(t)}$ and so on, and each time reach the same conclusion: they involve a linear part made of operators L, L' , etc. and a remainder that is higher order. The specific form of the operator L appearing in (2.22) is given by its action on any function $g : D \times \mathbb{R} \rightarrow \mathbb{R}$

$$(2.23) \quad \begin{aligned} Lg(\mathbf{y}, c) = & \nabla \cdot \left(\rho_0(t, \mathbf{y}, c) \nabla \frac{\delta \mathcal{E}_0[g]}{\delta g} \right) + \partial_c \cdot \left(\rho_0(t, \mathbf{y}, c) \partial_c \frac{\delta \mathcal{E}_0[g]}{\delta g} \right) \\ & + \nabla \cdot \left(\nabla (F_0(t, \mathbf{y}) - F(\mathbf{y})) c g \right) + \partial_c \left((F_0(t, \mathbf{y}) - F(\mathbf{y})) g \right) \end{aligned}$$

where \mathcal{E}_0 is defined in (2.12) and $F_0(t)$ in (2.13). The gradient part in this operator implies that it is dissipative, which in turns means that in (2.22) the linear term $L \tilde{\rho}_{\xi(t)}$ damps the effect of the source $R_{\xi(t)}$ and of $\dot{\xi}(t) \log n \tilde{\rho}_{\xi(t)}$. Since this source term itself satisfies an equation where the linear term damps the effect of the source, and so on, we can formally conclude that each of the terms $n^{-\xi(t)} \tilde{\rho}_{\xi(t)} \tilde{\rho}'_{\xi(t)}$, $n^{-2\xi(t)} \tilde{\rho}_{\xi(t)} \tilde{\rho}'_{\xi(t)} \tilde{\rho}''_{\xi(t)}$, etc. will remain at all times $t > 0$ on the scale set by \mathbb{P}_{in} .

This argument implies that, as long as (2.20) holds and $\xi(t) < 1$ at all times, $\tilde{\rho}_{\xi(t)}$ will have a limit as $n \rightarrow \infty$. If we take this limit at any fixed time, then (2.20) will imply that $\xi(t) = \xi(0) = \frac{1}{2}$ as $n \rightarrow \infty$, that is, we will have remained on the original scale set by \mathbb{P}_{in} . On that scale, we have $\tilde{\rho}_{1/2}(t) \rightarrow \rho_{1/2}(t)$ as $n \rightarrow \infty$, where $\rho_{1/2}(t)$ solves

$$(2.24) \quad \begin{aligned} \partial_t \rho_{1/2} = & \nabla \cdot \left(-c \nabla F \rho_{1/2} + \int_{D \times \mathbb{R}} c c' \nabla K(\mathbf{y}, \mathbf{y}') (\rho'_{1/2} \rho_0 + \rho'_0 \rho_{1/2}) d\mathbf{y}' d\mathbf{c}' \right) \\ & + \partial_c \left(-F \rho_{1/2} + \int_{D \times \mathbb{R}} c' K(\mathbf{y}, \mathbf{y}') (\rho'_{1/2} \rho_0 + \rho'_0 \rho_{1/2}) d\mathbf{y}' d\mathbf{c}' \right) \end{aligned}$$

this equation should be solved with the Gaussian initial conditions read from (2.18):

$$(2.25) \quad \rho_{1/2}(0, \mathbf{y}, c) = N(0, \rho_{\text{in}}(\mathbf{y}, c) \delta(\mathbf{y} - \mathbf{y}') \delta(c - c')).$$

Note that since the mean of $\rho_{1/2}$ is zero initially and (2.24) is linear, this mean remains zero for all times, and we can focus in the evolution of its covariance. Denoting this covariance by

$$(2.26) \quad \omega_{1/2}(t, \mathbf{y}, c, \mathbf{y}', c') = \mathbb{E}_{\text{in}} \rho_{1/2}(t, \mathbf{y}, c) \rho_{1/2}(t, \mathbf{y}', c'),$$

from (2.24) it satisfies

$$(2.27) \quad \begin{aligned} \partial_t \omega_{1/2} = & \nabla \cdot \left(-c \nabla F \omega_{1/2} + \int_{D \times \mathbb{R}} c c'' \nabla K(\mathbf{y}, \mathbf{y}'') (\omega_{1/2} \rho_0 + \omega_{1/2} \rho_0'') d\mathbf{y}'' dc'' \right) \\ & + \partial_c \left(-F \omega_{1/2} + \int_{D \times \mathbb{R}} c' K(\mathbf{y}, \mathbf{y}'') (\omega_{1/2} \rho_0 + \omega_{1/2} \rho_0'') d\mathbf{y}'' dc'' \right) \\ & + \nabla' \cdot \left(-c' \nabla' F' \omega_{1/2} + \int_{D \times \mathbb{R}} c' c'' \nabla K(\mathbf{y}, \mathbf{y}'') (\omega_{1/2} \rho_0' + \omega_{1/2} \rho_0'') d\mathbf{y}'' dc'' \right) \\ & + \partial_{c'} \left(-F' \omega_{1/2} + \int_{D \times \mathbb{R}} c'' K(\mathbf{y}', \mathbf{y}'') (\omega_{1/2} \rho_0' + \omega_{1/2} \rho_0'') d\mathbf{y}'' dc'' \right) \end{aligned}$$

where we use the shorthands $\omega_{1/2} \rho_0 = \omega_{1/2}(t, \mathbf{y}', c', \mathbf{y}'', c'') \rho_0(t, \mathbf{y}, c)$, $\omega_{1/2} \rho_0' = \omega_{1/2}(t, \mathbf{y}'', c'', \mathbf{y}, c) \rho_0(t, \mathbf{y}', c')$, and $\omega_{1/2} \rho_0'' = \omega_{1/2}(t, \mathbf{y}, c, \mathbf{y}', c') \rho_0(t, \mathbf{y}'', c'')$. The initial condition for (2.27) is

$$(2.28) \quad \omega_{1/2}(0, \mathbf{y}, c, \mathbf{y}', c') = \rho_{\text{in}}(\mathbf{y}, c) \delta(\mathbf{y} - \mathbf{y}') \delta(c - c').$$

The existence of the weak limit of $\bar{\rho}_{1/2}$ even with $\xi(t) = \xi(0) = \frac{1}{2}$ is enough to confirm that $\rho_n(t) \rightharpoonup \rho_0(t)$ as $n \rightarrow \infty$, where $\rho_0(t)$ solves (2.9). However, we would like to consider different values of $\xi(t)$ to get a better handle on the size of the fluctuations at long times. In practice this can be done by choosing, for example,

$$(2.29) \quad \xi(t) = \bar{\xi}(t/a_n) \quad \text{with} \quad \lim_{n \rightarrow \infty} a_n / \log n = \infty, \quad \bar{\xi}(0) = \frac{1}{2}, \quad \bar{\xi}(s) < 1 \quad \forall s > 0$$

so that $\dot{\xi}(t) = \bar{\xi}'(t/a_n)/a_n$ and satisfies (2.20). If we then set the time to be $a_n + t$, we can conclude that $\bar{\rho}_{\xi(a_n+t)}(a_n + t) \rightharpoonup \rho_{\bar{\xi}}(t)$, where $\bar{\xi} = \bar{\xi}(1)$ and $\rho_{\bar{\xi}}(t)$ solves

$$(2.30) \quad \begin{aligned} \partial_t \rho_{\bar{\xi}} = & \nabla \cdot \left(-c \nabla F \rho_{\bar{\xi}} + \int_{D \times \mathbb{R}} c c' \nabla K(\mathbf{y}, \mathbf{y}') (\rho_{\bar{\xi}}' \rho_0 + \rho_0' \rho_{\bar{\xi}}) d\mathbf{y}' dc' \right) \\ & + \partial_c \left(-F \rho_{\bar{\xi}} + \int_{D \times \mathbb{R}} c' K(\mathbf{y}, \mathbf{y}') (\rho_{\bar{\xi}}' \rho_0 + \rho_0' \rho_{\bar{\xi}}) d\mathbf{y}' dc' \right) \end{aligned}$$

where ρ_0 in this equation is understood as $\lim_{n \rightarrow \infty} \rho_0(a_n + t)$, assuming that this limit exists (we will check in Sec. 2.3 that it does). Because of the way we have taken the limit to arrive at this equation, it is valid at times that are infinitely far in the future of the initial conditions. This changes the interpretation we need to give to (2.30): Since (2.30) is linear and homogeneous in $\rho_{\bar{\xi}}$, either zero is a stable fixed point of this equation, and it means that the size of the fluctuations at time $s \log n$ are bounded from above by $O(n^{-\bar{\xi}})$, with $\bar{\rho}_{\bar{\xi}}(s \log n + t) \rightarrow 0$; or zero is an unstable fixed point of (2.30), and these fluctuations go to infinity even on the scale $O(n^{-1/2})$. In Sec. 2.4 we will check that the former statement holds. Note that in that case, it means we can take $\bar{\xi}$ as large as we want in $[1/2, 1)$.

Summing up, we have obtained:

Proposition 2.1. *Let $\rho_n(t)$ be the empirical distribution in (2.3) in which $\{\mathbf{Y}_i(t), C_i(t)\}_{i=1}^n$ solve (2.1) with initial conditions drawn from \mathbb{P}_{in} . Then, as $n \rightarrow \infty$:*

$$(2.31) \quad \rho_n(t, \mathbf{y}, c) \rightharpoonup \rho_0(t, \mathbf{y}, c), \quad \text{almost surely}$$

where $\rho_0(t)$ solves (2.9), and

$$(2.32) \quad n^{1/2} (\bar{\rho}_{1/2}(t, \mathbf{y}, c) - \rho_0(t, \mathbf{y}, c)) \rightharpoonup \rho_{1/2}(t, \mathbf{y}, c), \quad \text{in law}$$

where $\rho_{1/2}(t)$ is the zero-mean Gaussian process whose covariance $\omega_\xi(t)$ solves (2.27). In addition, if zero is the stable fixed point of (2.30), then

$$(2.33) \quad n^{\bar{\xi}} \left(\tilde{\rho}_\xi(a_n, \mathbf{y}, c) - \rho_0(a_n, \mathbf{y}, c) \right) \rightarrow 0, \quad \text{almost surely}$$

for any $\bar{\xi} < 1$ and a_n such that $a_n / \log n \rightarrow \infty$ as $n \rightarrow \infty$.

Note that we have yet to check that the condition that leads to (2.33) can be satisfied: we will do this in Sec. 2.4.

Remark 2.1. The argument that led us to conclude that in (2.19) the term $n^{-\xi} \tilde{\rho}_\xi \tilde{\rho}'_\xi$ converges to zero almost surely if $\xi < 1$ is related to the property of *propagation of molecular chaos*. This property holds if \mathbb{P}_{in} being a product measure implies that its push-forward in time is also a product measure, and it guarantees that $n^{-\xi} \tilde{\rho}_\xi \tilde{\rho}'_\xi = O(n^{\xi-1})$

Remark 2.2. In order that (2.15) have a limit at $t = 0$ for initial condition drawn from \mathbb{P}_{in} it is required that $\xi(0) < \frac{1}{2}$. At the same time, $n^{-\xi} \tilde{\rho}_\xi \tilde{\rho}'_\xi \rightarrow 0$ as $n \rightarrow \infty$ only requires that $\xi < 1$. This is why we were allowed to vary $\xi(t)$ slowly with time in a way consistent with (2.29), and it shows that the fluctuations present in the initial data diminish as time progresses. We will revisit the consequences of this property in Sec. 2.4.

2.3. Law of Large Numbers (LLN). Let us now analyze the evolution equation (2.9) for the weak limit ρ_0 of ρ_n . To begin notice that (2.9) can be used to derive a closed equation for

$$(2.34) \quad f_0(t, \mathbf{x}) = \int_{D \times \mathbb{R}} c \varphi(\mathbf{x}, \mathbf{y}) \rho_0(t, \mathbf{y}, c) d\mathbf{y} dc$$

Indeed, we can write (2.9) as

$$(2.35) \quad \begin{aligned} \partial_t \rho_0 &= \nabla \cdot \left(c \int_{\Omega} \nabla_{\mathbf{y}} \varphi(\mathbf{x}, \mathbf{y}) (f_0(t, \mathbf{x}) - f(\mathbf{x})) d\mu(\mathbf{x}) \rho_0 \right) \\ &\quad + \partial_c \left(\int_{\Omega} \varphi(\mathbf{x}, \mathbf{y}) (f_0(t, \mathbf{x}) - f(\mathbf{x})) d\mu(\mathbf{x}) \rho_0 \right) \end{aligned}$$

from which we deduce, using (2.34),

$$(2.36) \quad \begin{aligned} \partial_t f_0(t, \mathbf{x}) &= \int_{D \times \mathbb{R}} c \varphi(\mathbf{x}, \mathbf{y}) \partial_t \rho_0(t, \mathbf{y}, c) d\mathbf{y} dc \\ &= \int_{D \times \mathbb{R}} c \varphi(\mathbf{x}, \mathbf{y}) \nabla \cdot \left(c \int_{\Omega} \nabla_{\mathbf{y}} \varphi(\mathbf{x}, \mathbf{y}) (f_0(t, \mathbf{x}) - f(\mathbf{x})) d\mu(\mathbf{x}) \rho_0 \right) d\mathbf{y} dc \\ &\quad + \int_{D \times \mathbb{R}} c \varphi(\mathbf{x}, \mathbf{y}) \partial_c \left(\int_{\Omega} \varphi(\mathbf{x}, \mathbf{y}) (f_0(t, \mathbf{x}) - f(\mathbf{x})) d\mu(\mathbf{x}) \rho_0 \right) d\mathbf{y} dc \end{aligned}$$

By integrating by parts in \mathbf{y} the first term and in c the second, and interchanging the order of integration between (\mathbf{y}, c) and \mathbf{x} on both these terms, this equation can be written as

$$(2.37) \quad \partial_t f_0(t, \mathbf{x}) = - \int_{\Omega} M([\rho_0(t)], \mathbf{x}, \mathbf{x}') (f_0(t, \mathbf{x}') - f(\mathbf{x}')) d\mu(\mathbf{x}')$$

where we defined the kernel

$$(2.38) \quad M([\rho], \mathbf{x}, \mathbf{x}') = \int_{D \times \mathbb{R}} (c^2 \nabla_{\mathbf{y}} \varphi(\mathbf{x}, \mathbf{y}) \nabla_{\mathbf{y}} \varphi(\mathbf{x}', \mathbf{y}) + \varphi(\mathbf{x}, \mathbf{y}) \varphi(\mathbf{x}', \mathbf{y})) \rho(\mathbf{y}, c) d\mathbf{y} dc.$$

This kernel is symmetric in \mathbf{x} and \mathbf{x}' , and positive-definite for any probability density function $\rho > 0$ since, given any $r \in L^2(\Omega, \mu)$, we have

$$(2.39) \quad \int_{\Omega^2} r(\mathbf{x}) r(\mathbf{x}') M([\rho], \mathbf{x}, \mathbf{x}') d\mu(\mathbf{x}) d\mu(\mathbf{x}') = \int_{D \times \mathbb{R}} (c^2 |\nabla R(\mathbf{y})|^2 + |R(\mathbf{y})|^2) \rho(\mathbf{y}, c) d\mathbf{y} dc$$

where

$$(2.40) \quad R(\mathbf{y}) = \int_{\Omega} r(\mathbf{x}) \varphi(\mathbf{x}, \mathbf{y}) d\mu(\mathbf{x}).$$

As a result, (2.39) is non-negative and it can only be zero if $R = 0$ a.e. in D . By Assumption 1.3 this requires $r = 0$ a.e. in Ω , which shows that $M([\rho], \mathbf{x}, \mathbf{x}')$ is positive-definite. This also implies that the only stable fixed point of (2.37) is f . In other words, since $f_0(t)$ is the limit of $f_n(t)$ as $n \rightarrow \infty$, we have formally established:

Proposition 2.2 (LLN). *Let $f_n(t) = f_n(t, \mathbf{x})$ be given by (2.4) with $\{\mathbf{Y}_i(t), C_i(t)\}_{i=1}^n$ solution of (2.1) with initial condition drawn from \mathbb{P}_{in} . Then*

$$(2.41) \quad \lim_{n \rightarrow \infty} f_n(t) = f_0(t) \quad \mathbb{P}_{in}\text{-almost surely}$$

where $f_0(t)$ solves (2.37) and satisfies

$$(2.42) \quad \lim_{t \rightarrow \infty} f_0(t) = f \quad \text{a.e. in } \Omega$$

Note that this result also indicates that, for large n , the rate in time at which $f_n(t)$ converges towards f is independent of n to leading order, since n does not enter (2.37). In addition, this result confirms that $f_0(t)$ evolves on a quadratic landscape, namely the loss function (1.2) itself: Indeed (2.37) can be written as

$$(2.43) \quad \partial_t f_0(t, \mathbf{x}) = - \int_{\Omega} M([\rho_0(t)], \mathbf{x}, \mathbf{x}') D_{f_0(t, \mathbf{x}')} \ell(f, f_0) d\mu(\mathbf{x}')$$

where $D_{f(\mathbf{x})}$ denotes the gradient with respect to $f(\mathbf{x})$ in the $L^2(\Omega, \mu)$ -norm, i.e. given a functional $\mathcal{F}[f]$,

$$(2.44) \quad \forall h : \Omega \rightarrow \mathbb{R} \quad : \quad \lim_{z \rightarrow 0} \frac{d}{dz} \mathcal{F}[f + zh] = \langle h, D_f \mathcal{F}[f] \rangle_{L^2(\Omega, \mu)} = \int_{\Omega} h(\mathbf{x}) D_{f(\mathbf{x})} \mathcal{F}[f] d\mu(\mathbf{x})$$

(That is, $D_{f(\mathbf{x})}$ reduces to $\delta/\delta f(\mathbf{x})$ if $d\mu(\mathbf{x}) = d\mathbf{x}$.)

Even though the argument above specifies fully the asymptotic behavior of $\lim_{n \rightarrow \infty} f_n(t)$ as $t \rightarrow \infty$, it gives incomplete information about that of $\lim_{n \rightarrow \infty} \rho_n(t) = \rho_0(t)$: we only know that this limiting $\rho_0(t)$ is such that $\int_{D \times \mathbb{R}} c \varphi(\mathbf{x}, \mathbf{y}) \rho_0(t, \mathbf{y}, c) d\mathbf{y} dc$ converges to $f(\mathbf{x})$ as $t \rightarrow \infty$. This is corroborated by the fact that the minimizer of (2.11) subject to $\int_{D \times \mathbb{R}} \rho_0(\mathbf{y}, c) d\mathbf{y} dc = 1$ is not necessarily unique, since the Euler-Lagrange equation for this minimization problem reads

$$(2.45) \quad -cF + c \int_{D \times \mathbb{R}} c' K(\mathbf{y}, \mathbf{y}') \rho_0(\mathbf{y}', c') d\mathbf{y}' dc' = A_0$$

where A_0 is a constant added to enforce the constraint. Setting $c = 0$ in this equation indicates that $A_0 = 0$, which means that we can divide both sides by c . The resulting equation is a closed equation for $G_0(\mathbf{y}) := \int_{\mathbb{R}} c \rho_0(\mathbf{y}, c) dc$:

$$(2.46) \quad -F + \int_D K(\mathbf{y}, \mathbf{y}') G_0(\mathbf{y}') d\mathbf{y}' = 0$$

This equation is precisely (1.15), and we know that for any solution G_0^* we have

$$(2.47) \quad f = \int_D \varphi(\cdot, \mathbf{y}) G_0^*(\mathbf{y}) d\mathbf{y} \quad \text{a.e. in } \Omega$$

which confirms the result in Proposition 2.2 but does not indicate which fixed point $\rho_0(t)$ will reach.

2.4. Central Limit Theorem (CLT). Let us now analyze (2.30). Notice first that since $F_0(t) \rightarrow F$ as $t \rightarrow \infty$, on the time scales where this equation holds, it reduces to

$$(2.48) \quad \partial_t \rho_{\xi} = \nabla \cdot \left(\int_{D \times \mathbb{R}} c c' \nabla K(\mathbf{y}, \mathbf{y}') \rho'_{\xi} \rho_0 d\mathbf{y}' dc' \right) + \partial_c \left(\int_{D \times \mathbb{R}} c' K(\mathbf{y}, \mathbf{y}') \rho'_{\xi} \rho_0 d\mathbf{y}' dc' \right)$$

in which ρ_0 is the fixed point reached by (2.9). Proceeding as we did to derive (2.37) we can write an equation for

$$(2.49) \quad f_{\xi}(t, \mathbf{x}) = \int_{D \times \mathbb{R}} c \varphi(\mathbf{x}, \mathbf{y}) \rho_{\xi}(t, \mathbf{y}, c) d\mathbf{y} dc$$

which is

$$(2.50) \quad \partial_t f_{\bar{\xi}} = - \int_{\Omega} M([\rho_0(t)], \mathbf{x}, \mathbf{x}') f_{\bar{\xi}}(t, \mathbf{x}') d\mu(\mathbf{x}')$$

where $M([\rho], \mathbf{x}, \mathbf{x}')$ is the kernel defined in (2.38). Since $M([\rho], \mathbf{x}, \mathbf{x})$ is positive-definite, the only fixed point of (2.50) is zero, and

$$(2.51) \quad \lim_{t \rightarrow \infty} f_{\bar{\xi}}(t) = 0.$$

This also implies that $\rho_{\bar{\xi}} = 0$ is a stable fixed point of (2.48), which was the condition for (2.33) to hold.

Summarizing we have established:

Proposition 2.3 (CLT). *Let $f_n(t) = f_n(t, \mathbf{x})$ be given by (2.4) with $\{\mathbf{Y}_i(t), C_i(t)\}_{i=1}^n$ solution of (2.1) with initial condition drawn from \mathbb{P}_{in} . Then for any $\bar{\xi} < 1$ and any $a_n > 0$ such that $a_n / \log n \rightarrow \infty$ as $n \rightarrow \infty$, we have*

$$(2.52) \quad \lim_{n \rightarrow \infty} n^{\bar{\xi}} (f_n(a_n) - f_0(a_n)) = 0 \quad \text{in law}$$

where $f_0(t)$ solves (2.37) and satisfies $f_0(t) \rightarrow f$ as $t \rightarrow \infty$, and

This proposition can be stated as (1.21). It shows a remarkable self-healing property of the dynamics: the fluctuations at scale $O(n^{-1/2})$ of $f_n(t)$ around $f_0(t)$ that were present initially decrease in amplitude as time progresses, and become $o(n^{-1})$ as $t \rightarrow \infty$.

Finally, note that the results above have consequences in terms of the scaling of the loss function. We can write

$$(2.53) \quad \ell(f, f_n(a_n)) = \frac{1}{2} \|f - f_0(a_n)\|^2 - n^{-\bar{\xi}} \langle f - f_0(a_n), f_{\bar{\xi}}(a_n) \rangle + \frac{1}{2} n^{-2\bar{\xi}} \|f_{\bar{\xi}}(a_n)\|^2 + o(n^{-\bar{\xi}})$$

where the norms and inner products are taken in $L^2(\Omega, \mu)$ and we denote $f_0(t) \rightarrow f$ and $f_{\bar{\xi}}(t) \rightarrow 0$ as $t \rightarrow \infty$, we deduce

Proposition 2.4. *In the same conditions as those in Proposition 2.3, the loss function satisfies*

$$(2.54) \quad \lim_{n \rightarrow \infty} n^{\bar{\xi}} \ell(f, f_n(a_n)) = 0 \quad \text{almost surely.}$$

3. FINITE TRAINING SET AND STOCHASTIC GRADIENT DESCENT (SGD)

In most applications, it is not possible to evaluate the integrals in (1.4) defining $F(\mathbf{y})$ and $K(\mathbf{y}, \mathbf{z})$. This is especially true for $F(\mathbf{y})$, since we typically have limited access to $f(\mathbf{x})$: often, we only know its value on a finite set of points. In these cases, unless we use radial basis function networks (as discussed in Sec. 4.1) we need to approximate the integrals in (1.4) by sum over a finite set of \mathbf{x} 's by sampling from the measure μ . Typically, this sampling is done at every step of the learning process, which introduce some noise, and the resulting scheme is referred to as stochastic gradient descent. The noise in this scheme can be used to replace the noise terms in (2.1): here we discuss in which way this modification impacts the results established before.

The SGD scheme used to train the network in applications reads

$$(3.1) \quad \begin{cases} \mathbf{Y}_i^P(t + \Delta t) = \mathbf{Y}_i^P(t) + C_i^P(t) \nabla F_P(t, \mathbf{Y}_i^P(t)) \Delta t - \frac{1}{n} \sum_{j=1}^n C_j^P(t) C_j^P(t) \nabla K_P(t, \mathbf{Y}_i^P(t), \mathbf{Y}_j^P(t)) \Delta t \\ C_i^P(t + \Delta t) = C_i(t) + F_P(t, \mathbf{Y}_i^P(t)) \Delta t - \frac{1}{n} \sum_{j=1}^n C_j^P(t) K_P(t, \mathbf{Y}_i^P(t), \mathbf{Y}_j^P(t)) \Delta t \end{cases}$$

where $\Delta t > 0$ is some time-step and we defined

$$(3.2) \quad F_P(t, \mathbf{y}) = \frac{1}{P} \sum_{p=1}^P f(\mathbf{X}_p(t)) \varphi(\mathbf{X}_p(t), \mathbf{y}), \quad K_P(t, \mathbf{y}, \mathbf{y}') = \frac{1}{P} \sum_{p=1}^P \varphi(\mathbf{X}_p(t), \mathbf{y}) \varphi(\mathbf{X}_p(t), \mathbf{y}')$$

in which $\{\mathbf{X}_p(t)\}_{p=1}^P$ are P iid variables which are redrawn from μ independently at every time step t .

3.1. Limiting stochastic differential equation (SDE). To analyze the properties of (3.1), it is convenient to use compact notations and denote the set of all particles as

$$(3.3) \quad \mathbf{z} = (\mathbf{z}_1, \dots, \mathbf{z}_n) = (\mathbf{y}_1, c_1, \dots, \mathbf{y}_n, c_n) \in (D \times \mathbb{R})^n, \quad \mathbf{z}_i = (\mathbf{y}_i, c_i) \in D \times \mathbb{R} \quad i = 1, \dots, n$$

and use the shorthands

$$(3.4) \quad f_n(\mathbf{z}) = \frac{1}{n} \sum_{i=1}^n c_i \varphi(\cdot, \mathbf{y}_i), \quad f_n(\mathbf{x}, \mathbf{z}) = \frac{1}{n} \sum_{i=1}^n c_i \varphi(\mathbf{x}, \mathbf{y}_i)$$

The stochastic gradient descent in (3.1) can be written as

$$(3.5) \quad \mathbf{Z}(t + \Delta t) = \mathbf{Z}(t) - \Delta t \nabla_{\mathbf{z}} L_P(\mathbf{Z}(t))$$

where $L_P(\mathbf{z})$ is the approximation of the loss function obtained with a batch of P independent samples $\{\mathbf{X}_p(t)\}_{p=1}^P$ drawn from μ and scaled by n :

$$(3.6) \quad L_P(\mathbf{z}) = \frac{n}{2P} \sum_{p=1}^P |f(\mathbf{X}_p) - f_n(\mathbf{X}_p, \mathbf{z})|^2$$

Notice that $L_P(\mathbf{z})$ has expectation $n\ell(f, f_n(\mathbf{z}))$:

$$(3.7) \quad \mathbb{E} L_P(\mathbf{z}) = \frac{n}{2} \int_{\Omega} |f(\mathbf{x}) - f_n(\mathbf{x}, \mathbf{z})|^2 d\mu(\mathbf{x}) = n\ell(f, f_n)$$

Note also that

$$(3.8) \quad \nabla_{\mathbf{z}} L_P(\mathbf{z}) = \frac{n}{P} \sum_{p=1}^P (f_n(\mathbf{X}_p, \mathbf{z}) - f(\mathbf{X}_p)) \nabla_{\mathbf{z}} f_n(\mathbf{X}_p, \mathbf{z})$$

Let us introduce the covariance of this quantity:

$$(3.9) \quad \mathbb{E} (\nabla_{\mathbf{z}} (L_P(\mathbf{z}) - n\ell(f, f_n(\mathbf{z})))) \otimes (\nabla_{\mathbf{z}} (L_P(\mathbf{z}') - n\ell(f, f_n(\mathbf{z}')))) = \frac{1}{P} R(\mathbf{z})$$

with

$$(3.10) \quad R(\mathbf{z}) = n^2 \int_{\Omega} |f(\mathbf{x}) - f_n(\mathbf{x}, \mathbf{z})|^2 \nabla_{\mathbf{z}} f_n(\mathbf{x}, \mathbf{z}) \otimes \nabla_{\mathbf{z}} f_n(\mathbf{x}, \mathbf{z}) d\mu(\mathbf{x}) - n^2 \nabla_{\mathbf{z}} \ell(f, f_n(\mathbf{z})) \otimes \nabla_{\mathbf{z}} \ell(f, f_n(\mathbf{z}))$$

It is useful in what follows to express the blocks of this tensor as

$$(3.11) \quad R_{i,j}(\mathbf{z}) = \begin{pmatrix} c_i c_j A_2(\llbracket f - f_n \rrbracket, \mathbf{y}_i, \mathbf{y}_j) & c_i A_1(\llbracket f - f_n \rrbracket, \mathbf{y}_i, \mathbf{y}_j) \\ c_j A_1(\llbracket f - f_n \rrbracket, \mathbf{y}_j, \mathbf{y}_i) & A_0(\llbracket f - f_n \rrbracket, \mathbf{y}_i, \mathbf{y}_j) \end{pmatrix}$$

where

$$(3.12) \quad \begin{aligned} A_0(\llbracket f \rrbracket, \mathbf{y}, \mathbf{y}') &= \int_{\Omega} |f(\mathbf{x})|^2 \varphi(\mathbf{x}, \mathbf{y}) \varphi(\mathbf{x}, \mathbf{y}') d\mu(\mathbf{x}) \\ &\quad - \int_{\Omega} f(\mathbf{x}) \varphi(\mathbf{x}, \mathbf{y}) d\mu(\mathbf{x}) \int_{\Omega} f(\mathbf{x}) \varphi(\mathbf{x}, \mathbf{y}') d\mu(\mathbf{x}) \\ A_1(\llbracket f \rrbracket, \mathbf{y}, \mathbf{y}') &= \int_{\Omega} |f(\mathbf{x})|^2 \nabla_{\mathbf{y}} \varphi(\mathbf{x}, \mathbf{y}) \varphi(\mathbf{x}, \mathbf{y}') d\mu(\mathbf{x}) \\ &\quad - \int_{\Omega} f(\mathbf{x}) \nabla_{\mathbf{y}} \varphi(\mathbf{x}, \mathbf{y}) d\mu(\mathbf{x}) \int_{\Omega} f(\mathbf{x}) \varphi(\mathbf{x}, \mathbf{y}') d\mu(\mathbf{x}) \\ A_2(\llbracket f \rrbracket, \mathbf{y}, \mathbf{y}') &= \int_{\Omega} |f(\mathbf{x})|^2 \nabla_{\mathbf{y}} \varphi(\mathbf{x}, \mathbf{y}) \otimes \nabla_{\mathbf{y}'} \varphi(\mathbf{x}, \mathbf{y}') d\mu(\mathbf{x}) \\ &\quad - \int_{\Omega} f(\mathbf{x}) \nabla_{\mathbf{y}} \varphi(\mathbf{x}, \mathbf{y}) d\mu(\mathbf{x}) \otimes \int_{\Omega} f(\mathbf{x}) \nabla_{\mathbf{y}'} \varphi(\mathbf{x}, \mathbf{y}') d\mu(\mathbf{x}) \end{aligned}$$

To keep track of the terms, note that $A_0 \in \mathbb{R}$, $A_1 \in \mathbb{R}^n$, and $A_2 \in \mathbb{R}^n \times \mathbb{R}^n$.

If in (3.5) we split $\nabla_{\mathbf{z}} L_P(\mathbf{Z})$ into its expectation plus a zero-mean fluctuations with covariance (3.9), we can think of (3.1) as an Euler-Maruyama scheme for an SDE, except that the scaling of the noise term is incorrect, since it involves Δt rather than $\sqrt{\Delta t}$. This SDE is

$$(3.13) \quad d\mathbf{Z} = n\nabla_{\mathbf{z}} \ell(f, f_n(\mathbf{Z})) dt + \sqrt{\theta} d\mathbf{B}$$

where $\theta = \Delta t/P$ and $d\mathbf{B}$ is a white-noise process with quadratic variation

$$(3.14) \quad \langle d\mathbf{B}, d\mathbf{B} \rangle = R(\mathbf{Z}) dt$$

In the original variables, (3.13) reads

$$(3.15) \quad \begin{cases} d\mathbf{Y}_i = C_i \nabla F(\mathbf{Y}_i) dt - \frac{1}{n} \sum_{j=1}^n C_i C_j \nabla K(\mathbf{Y}_i, \mathbf{Y}_j) dt + \sqrt{\theta} d\mathbf{B}_i, \\ dC_i = F(\mathbf{Y}_i) dt - \frac{1}{n} \sum_{j=1}^n C_j K(\mathbf{Y}_i, \mathbf{Y}_j) dt + \sqrt{\theta} dB'_i \end{cases}$$

where $\{d\mathbf{B}_i, dB'_i\}_{i=1}^n$ are a white-noise processes with quadratic variation

$$(3.16) \quad \begin{aligned} \langle d\mathbf{B}_i, d\mathbf{B}_j \rangle &= C_i C_j A_2([f - f_n], \mathbf{Y}_i, \mathbf{Y}_j) dt \\ \langle d\mathbf{B}_i, dB'_j \rangle &= C_i A_1([f - f_n], \mathbf{Y}_i, \mathbf{Y}_j) dt \\ \langle dB'_i, dB'_j \rangle &= A_0([f - f_n], \mathbf{Y}_i, \mathbf{Y}_j) dt \end{aligned}$$

Let us state more precisely how the solution to (3.1) is close to that of (3.15), in a way that is convenient for our purpose. Denote

$$(3.17) \quad f_n^P(t, \mathbf{x}) = \frac{1}{n} \sum_{i=1}^N C_i^P(t) \varphi(\mathbf{x}, \mathbf{Y}_i^P(t)), \quad f_n(t, \mathbf{x}) = \frac{1}{n} \sum_{i=1}^N C_i(t) \varphi(\mathbf{x}, \mathbf{Y}_i(t)),$$

where in the first sum we use the solution to (3.1) and in the second that of (3.15). Then we have [23, 24]

Proposition 3.1. *Given any test functions $\psi : \Omega \rightarrow \mathbb{R}$ and $H : \mathbb{R} \rightarrow \mathbb{R}$, and any $T > 0$, there is a constant $C > 0$ such that*

$$(3.18) \quad \sup_{0 \leq k\Delta t \leq T} \left| \mathbb{E}H \left(\int_{\Omega} \psi(\mathbf{x}) f_n(k\Delta t, \mathbf{x}) d\mu(\mathbf{x}) \right) - \mathbb{E}H \left(\int_{\Omega} \psi(\mathbf{x}) f_n^P(k\Delta t, \mathbf{x}) d\mu(\mathbf{x}) \right) \right| \leq C\Delta t.$$

This proposition is a direct consequence of the fact that (3.1) can be viewed as the Euler-Maruyama discretization scheme for (3.15), and this scheme has weak order of accuracy 1. Note that if we let $\Delta t \rightarrow 0$, (3.15) reduces to the ODEs in (2.1) since $\theta = \Delta t/P \rightarrow 0$ in that limit. We should stress, however, that this limit is not reached in practice since the scheme (3.1) is used at small but finite Δt . As we show below θ should in fact be small—we can also adjust the size of θ at fixed Δt by changing P , i.e., by changing the batch size.

3.2. Dean's equation for particles with correlated noise. Proposition 3.1 indicates that we can analyze the properties of (3.15) instead of that of (3.1). Dean's equation for the empirical distribution of the process defined by (3.15) can be derived as in Sec. 2.1, except that we need to take into account the effect of the extra drift terms and the noise terms in (3.15).

Applying Itô's formula to (2.3) when $\{\mathbf{Y}_i(t), C_i(t)\}_{i=1}^n$ satisfy (3.15), we arrive at

$$\begin{aligned}
d\rho_n(t, \mathbf{y}, c) = & -\frac{1}{n} \sum_{i=1}^n \delta(c - C_i) \nabla \delta(\mathbf{y} - \mathbf{Y}_i) \cdot d\mathbf{Y}_i \\
& - \frac{1}{n} \sum_{i=1}^n \partial_c \delta(c - C_i) \delta(\mathbf{y} - \mathbf{Y}_i) dC_i \\
(3.19) \quad & + \frac{\theta}{2n} \sum_{i=1}^n \delta(c - C_i) \nabla \nabla \delta(\mathbf{y} - \mathbf{Y}_i) : C_i C_i A_2([f - f_n], \mathbf{Y}_i, \mathbf{Y}_i) dt \\
& + \frac{\theta}{n} \sum_{i=1}^n \partial_c^2 \delta(c - C_i) \nabla \delta(\mathbf{y} - \mathbf{Y}_i) \cdot C_i A_1([f - f_n], \mathbf{Y}_i, \mathbf{Y}_i) dt \\
& + \frac{\theta}{2n} \sum_{i=1}^n \partial_c^2 \delta(c - C_i) \delta(\mathbf{y} - \mathbf{Y}_i) A_0([f - f_n], \mathbf{Y}_i, \mathbf{Y}_i) dt
\end{aligned}$$

We use (2.3) to write $d\mathbf{Y}_i$ and dC_i , the drift terms that emerge can be treated as we did to derive (2.5). The noise term in (3.19) is

$$(3.20) \quad -\frac{1}{n} \sum_{i=1}^n \delta(c - C_i) \nabla \delta(\mathbf{y} - \mathbf{Y}_i) \cdot d\mathbf{B}_i - \frac{1}{n} \sum_{i=1}^n \partial_c \delta(c - C_i) \delta(\mathbf{y} - \mathbf{Y}_i) dB_i$$

and it can be checked explicitly using (3.16) that its quadratic variation can be expressed as

$$\begin{aligned}
(3.21) \quad & \nabla \nabla' : (\rho_n(t, \mathbf{y}, c) \rho_n(t, \mathbf{y}', c') c c' A_2([f_n(t) - f], \mathbf{y}, \mathbf{y}')) dt \\
& + \partial_c \partial_{c'} (\rho_n(t, \mathbf{y}, c) \rho_n(t, \mathbf{y}', c') A_0([f_n(t) - f], \mathbf{y}, \mathbf{y}')) dt \\
& + \partial_c \nabla' \cdot (\rho_n(t, \mathbf{y}, c) \rho_n(t, \mathbf{y}', c') c' A_1([f_n(t) - f], \mathbf{y}', \mathbf{y})) dt \\
& + \partial_{c'} \nabla \cdot (\rho_n(t, \mathbf{y}, c) \rho_n(t, \mathbf{y}', c') c A_1([f_n(t) - f], \mathbf{y}, \mathbf{y}')) dt
\end{aligned}$$

With this calculation we obtain Dean's equation for the empirical distribution of the stochastic gradient descent process

$$\begin{aligned}
(3.22) \quad \partial_t \rho_n = & \nabla \cdot \left(-c \nabla F \rho_n + \int_{D \times \mathbb{R}} c c' \nabla K(\mathbf{y}, \mathbf{y}') \rho'_n \rho_n d\mathbf{y}' dc' \right) \\
& + \partial_c \left(-F \rho_n + \int_{D \times \mathbb{R}} c' K(\mathbf{y}, \mathbf{y}') \rho'_n \rho_n d\mathbf{y}' dc' \right) \\
& + \frac{1}{2} \theta \nabla \nabla : (\rho_n c^2 A_2([f_n(t) - f], \mathbf{y}, \mathbf{y})) + \frac{1}{2} \theta \partial_c^2 (\rho_n A_0([f_n(t) - f], \mathbf{y}, \mathbf{y})) \\
& + \theta \partial_c \nabla \cdot (\rho_n c A_1([f_n(t) - f], \mathbf{y}, \mathbf{y})) \\
& + \sqrt{\theta} \dot{\eta}_n(t, \mathbf{y}, c)
\end{aligned}$$

where $f_n(t)$ is given by (2.4), i.e. $f_n(t, \mathbf{x}) = \int_{D \times \mathbb{R}} c \varphi(\mathbf{x}, \mathbf{y}) \rho_0(t, \mathbf{y}, c) d\mathbf{y} dc$, and we defined the white-noise process $\dot{\eta}_n(t, \mathbf{y}, c)$ with quadratic variation in (3.21).

The first two terms at the right hand side of (3.22) are the same as those of (2.5). This is because these terms come from the drift terms in (3.15), which also coincide with those in (2.1). However, (3.22) also contains additional drift and the noise terms that were absent in (2.5). If we want to make these terms higher order so that the LLN established in Proposition 2.2 still applies, we must scale these terms with some inverse power of n . Specifically, we will set

$$(3.23) \quad \theta = an^{-2\alpha} \quad \text{for some } a > 0 \quad \text{and } \alpha > 0$$

This scaling can be achieved e.g. by choosing $P = O(n^{2\alpha})$, i.e. by increasing the batch size with n .

3.3. Limit behavior and fluctuations scaling in SGD. If we substitute $\theta = an^{-2\alpha}$ with $\alpha > 0$ and take the limit as $n \rightarrow \infty$ of (3.22), we formally conclude that $\rho_n \rightarrow \rho_0$, where ρ_0 solves the same deterministic equation (2.9) as before.

Turning our attention to the fluctuations of ρ_n around ρ_0 , notice that there are two sources of them: some are intrinsic to the discrete nature of the particles apparent in ρ_n , and scale initially

as $O(n^{-1/2})$ and eventually as $O(n^{-\bar{\xi}})$ for any $\bar{\xi} < 1$, as discussed in Sec. 2.2.2. Other fluctuations come from the noise term in (3.22), and scale as $O(n^{-\alpha})$ when (3.23) holds—note that the drift terms proportional to $\theta = an^{-2\alpha}$ in (3.22) always make higher order contributions.

As a result:

- if $\alpha \in (0, 1)$ the fluctuations due to the noise in (3.22) eventually dominate the intrinsic ones from discreteness, and to capture them we can introduce $n^\alpha(\rho_n - \rho_0)$, write an equation for this quantity, and take the limit as $n \rightarrow \infty$ it. This leads to the conclusion that $n^\alpha(\rho_n - \rho_0) \rightarrow \rho_\alpha$ which satisfies (compare (2.19))

$$(3.24) \quad \begin{aligned} \partial_t \rho_\alpha = & \nabla \cdot \left(-c \nabla F \rho_\alpha + \int_{D \times \mathbb{R}} cc' \nabla K(\mathbf{y}, \mathbf{y}') (\rho'_\alpha \rho_0 + \rho'_0 \rho_\alpha) d\mathbf{y}' dc' \right) \\ & + \partial_c \left(-F \rho_\alpha + \int_{D \times \mathbb{R}} c' K(\mathbf{y}, \mathbf{y}') (\rho'_\alpha \rho_0 + \rho'_0 \rho_\alpha) d\mathbf{y}' dc' \right) \\ & + \sqrt{a} \dot{\eta}_0(t, \mathbf{y}, c) \end{aligned}$$

in which $\dot{\eta}_0(t, \mathbf{y}, c)$ is a white-noise process with quadratic variation

$$(3.25) \quad \begin{aligned} \langle d\eta_0(t, \mathbf{y}, c), d\eta_0(t, \mathbf{y}', c') \rangle = & \nabla \nabla' : (\rho_0(t, \mathbf{y}, c) \rho_0(t, \mathbf{y}', c') cc' A_2([f_0(t) - f], \mathbf{y}, \mathbf{y}')) dt \\ & + \partial_c \partial_{c'} (\rho_0(t, \mathbf{y}, c) \rho_0(t, \mathbf{y}', c') A_0([f_0(t) - f], \mathbf{y}, \mathbf{y}')) dt \\ & + \partial_c \nabla' \cdot (\rho_0(t, \mathbf{y}, c) \rho_0(t, \mathbf{y}', c') c' A_1([f_0(t) - f], \mathbf{y}', \mathbf{y})) dt \\ & + \partial_{c'} \nabla \cdot (\rho_0(t, \mathbf{y}, c) \rho_0(t, \mathbf{y}', c') c A_1([f_0(t) - f], \mathbf{y}, \mathbf{y}')) dt. \end{aligned}$$

- If $\alpha \geq 1$, then the fluctuations due to the noise in (3.22) are always negligible compared to the intrinsic ones from discreteness, and we are back to the GD situation studied in Sec. 2.

3.4. Law of Large Number and Central Limit Theorem for SGD. When $\theta = an^{-2\alpha}$ with $\alpha > 0$, $\rho_n \rightarrow \rho_0$ as $n \rightarrow \infty$, where ρ_0 solves (2.9). This implies that $f_0(t, \mathbf{x}) = \int_{D \times \mathbb{R}} c\varphi(\mathbf{x}, \mathbf{y}) \rho_0(t, \mathbf{y}, c) d\mathbf{y} dc$ satisfies (2.37) and is such that $f_0(t) \rightarrow f$ as $t \rightarrow \infty$. That is, the LLN in Proposition 2.2 still holds if we use the solution of (3.29) in (2.4); in turns, this means that this proposition also holds up to discretization errors in Δt if we use the solution of (3.1) in (2.4). For further reference, notice that this also implies that the factors defined in (3.12) satisfy

$$(3.26) \quad \lim_{t \rightarrow \infty} A_k([f_0(t) - f], \mathbf{y}, \mathbf{y}') = 0, \quad k = 0, 1, 2.$$

We will use this key property repeatedly in the sequel.

To analyze the fluctuations, let us focus on the situation where SGD differs from GD, i.e. $\alpha \in (0, 1)$, and write both (3.24) as

$$(3.27) \quad \begin{aligned} \partial_t \rho_\alpha = & \nabla \cdot \left(c \int_{\Omega} \nabla_{\mathbf{y}} \varphi(\mathbf{x}, \mathbf{y}) (f_0(t, \mathbf{x}) - f(\mathbf{x})) d\mu(\mathbf{x}) \rho_\alpha \right) \\ & + \partial_c \left(\int_{\Omega} \varphi(\mathbf{x}, \mathbf{y}) (f_0(t, \mathbf{x}) - f(\mathbf{x})) d\mu(\mathbf{x}) \rho_\alpha \right) \\ & + \nabla \cdot \left(c \int_{\Omega} \nabla_{\mathbf{y}} \varphi(\mathbf{x}, \mathbf{y}) f_\alpha(t, \mathbf{x}) d\mu(\mathbf{x}) \rho_0 \right) + \partial_c \left(\int_{\Omega} \varphi(\mathbf{x}, \mathbf{y}) f_\alpha(t, \mathbf{x}) d\mu(\mathbf{x}) \rho_0 \right) \\ & + \sqrt{a} \dot{\eta}_0(t, \mathbf{y}, c) \end{aligned}$$

where we defined

$$(3.28) \quad f_\alpha(t, \mathbf{x}) = \int_{D \times \mathbb{R}} c\varphi(\mathbf{x}, \mathbf{y}) \rho_\alpha(t, \mathbf{y}, c) d\mathbf{y} dc$$

This equation is structurally similar to (2.30) except that it also contains a noise term. By proceeding similarly as we did to derive (2.50) it leads to the following equation for $f_\alpha(t, \mathbf{x})$:

$$(3.29) \quad \begin{aligned} \partial_t f_\alpha &= - \int_{\Omega} M([\rho_0(t)], \mathbf{x}, \mathbf{x}') f_\alpha(t, \mathbf{x}') d\mu(\mathbf{x}') \\ &\quad - \int_{\Omega} M([\rho_\alpha(t)], \mathbf{x}, \mathbf{x}') (f_0(t, \mathbf{x}') - f(\mathbf{x}')) d\mu(\mathbf{x}') + \sqrt{a} \dot{\eta}(t, \mathbf{x}) \end{aligned}$$

where $M([\rho], \mathbf{x}, \mathbf{x}')$ is given in (2.38), and the quadratic variation of $\dot{\eta}(t, \mathbf{x})$ is precisely that of

$$(3.30) \quad \int_{D \times \mathbb{R}} c \varphi(\mathbf{x}, \mathbf{y}) \dot{\eta}_0(t, \mathbf{y}, c) d\mathbf{y} dc$$

and given by

$$(3.31) \quad \begin{aligned} \langle d\eta(t, \mathbf{x}), d\eta(t, \mathbf{x}') \rangle &= \int_{\Omega} N([\rho_0(t)], \mathbf{x}, \mathbf{x}', \bar{\mathbf{x}}, \bar{\mathbf{x}}) |f_0(t, \bar{\mathbf{x}}) - f(\bar{\mathbf{x}})|^2 d\mu(\bar{\mathbf{x}}) dt \\ &\quad - \int_{\Omega^2} N([\rho_0(t)], \mathbf{x}, \mathbf{x}', \bar{\mathbf{x}}, \bar{\mathbf{x}}') (f_0(t, \bar{\mathbf{x}}) - f(\bar{\mathbf{x}})) (f_0(t, \bar{\mathbf{x}}') - f(\bar{\mathbf{x}}')) d\mu(\bar{\mathbf{x}}) d\mu(\bar{\mathbf{x}}') dt \end{aligned}$$

in which

$$(3.32) \quad \begin{aligned} N([\rho], \mathbf{x}, \mathbf{x}', \bar{\mathbf{x}}, \bar{\mathbf{x}}') &= \int_{(D \times \mathbb{R}^2)} \rho(\mathbf{y}, c) \rho(\mathbf{y}', c') (c^2 \nabla_{\mathbf{y}} \varphi(\mathbf{x}, \mathbf{y}) \cdot \nabla_{\mathbf{y}} \varphi(\bar{\mathbf{x}}, \mathbf{y}) + \varphi(\mathbf{x}, \mathbf{y}) \varphi(\bar{\mathbf{x}}, \mathbf{y})) \\ &\quad \times (c'^2 \nabla_{\mathbf{y}'} \varphi(\mathbf{x}', \mathbf{y}') \cdot \nabla_{\mathbf{y}'} \varphi(\bar{\mathbf{x}}', \mathbf{y}') + \varphi(\mathbf{x}', \mathbf{y}') \varphi(\bar{\mathbf{x}}', \mathbf{y}')) d\mathbf{y} dc d\mathbf{y}' dc' \end{aligned}$$

The SDE (3.29) has the property that it *self-quenches* as $t \rightarrow \infty$: in that limit we know that $f_0(t) \rightarrow f$ and from (3.26) we see that $\dot{\eta}(t) \rightarrow 0$ as well. Therefore, at long times (3.29) reduces to

$$(3.33) \quad \partial_t f_\alpha = - \int_{\Omega} M([\rho_0(t)], \mathbf{x}, \mathbf{x}') f_\alpha(t, \mathbf{x}') d\mu(\mathbf{x}')$$

Since $M([\rho], \mathbf{x}, \mathbf{x}')$ is positive-definite the only (stable) fixed point of this equation is zero and $f_\alpha(t) \rightarrow 0$ as $t \rightarrow \infty$. Of course, to guarantee that this result holds, we should be on a long time scale such that the intrinsic fluctuations discussed in Sec. 2.4 have become higher order, i.e. $t = O(a_n)$ with $a_n > 0$ such that $a_n / \log n \rightarrow \infty$ as $n \rightarrow \infty$.

We can summarize this result as:

Proposition 3.2 (CLT for SGD). *Let $f_n(t) = f_n(t, \mathbf{x})$ be as in (2.4) with $\{\mathbf{Y}_i(t), C_i(t)\}_{i=1}^n$ solution to (3.15) with $\theta = an^{-2\alpha}$, $a > 0$, $\alpha \in (0, 1)$. Then for any $a_n > 0$ such that $a_n / \log n \rightarrow \infty$ as $n \rightarrow \infty$, we have*

$$(3.34) \quad \lim_{n \rightarrow \infty} n^\alpha (f_n(a_n) - f_0(a_n)) = 0 \quad \text{almost surely}$$

where $f_0(t)$ solves (2.37) and is such that $f_0(t) \rightarrow f$ as $t \rightarrow \infty$

In this statement, the almost sure convergence is with respect to \mathbb{P}_{in} as well as the statistics of the noise terms in (3.15). A similar statement holds if we use to the solution to (3.1) in $f_n(t) = f_n(t, \mathbf{x})$, but in this case discretization errors in Δt must also be accounted for. In terms of the loss function, we have

$$(3.35) \quad \ell(f, f_n(a_n)) = \frac{1}{2} \|f - f_0(a_n)\|^2 - n^{-\alpha} \langle f - f_0(a_n), f_\alpha(a_n) \rangle + \frac{1}{2} n^{-2\alpha} \|f_\alpha(a_n)\|^2 + o(n^{-\alpha})$$

and as a result we have the equivalent of Proposition 2.4 in the context of SGD

Proposition 3.3. *In the same conditions as those in Proposition 3.2, the loss function satisfies*

$$(3.36) \quad \lim_{t \rightarrow \infty} \lim_{n \rightarrow \infty} n^\alpha \ell(f, f_n(a_n)) = 0 \quad \text{almost surely}$$

4. ILLUSTRATIVE EXAMPLE: 3-SPIN MODEL ON THE HIGH-DIMENSIONAL SPHERE

To test our results, we will use a function known for its complex features in high-dimensions: the spherical 3-spin model, $f : S^{d-1}(\sqrt{d}) \rightarrow \mathbb{R}$, given by

$$(4.1) \quad f(\mathbf{x}) = \frac{1}{d} \sum_{p,q,r=1}^d a_{p,q,r} x_p x_q x_r, \quad \mathbf{x} \in S^{d-1}(\sqrt{d}) \subset \mathbb{R}^d$$

where the coefficients $\{a_{p,q,r}\}_{p,q,r=1}^d$ are independent Gaussian random variables with mean zero and unit variance. The function (4.1) is known to have a number of critical points that grows exponentially with the dimensionality d [13, 25, 26]. We note that previous works have sought to draw a parallel between the glassy 3-spin function and generic loss functions [14], but we are not exploring such an analogy here. Rather, we simply use the function (4.1) as a difficult target for approximation by neural networks. That is, throughout this section, we train networks to learn f with a particular realization of $a_{p,q,r}$ and study the accuracy of that representation as a function of the number of particles n .

4.1. Learning with Gaussian kernels. We first consider the case when $D = S^{d-1}(\sqrt{d})$ and we use

$$(4.2) \quad \varphi(\mathbf{x}, \mathbf{y}) = e^{-\frac{1}{2}\alpha|\mathbf{x}-\mathbf{y}|^2}$$

for some fixed $\alpha > 0$. In this case, the parameters live in the domain of the function (here the d -dimensional sphere). Note that, since $|\mathbf{x}| = |\mathbf{y}| = \sqrt{d}$, up to an irrelevant constant that can be absorbed in the weights c , we can also write (4.2) as

$$(4.3) \quad \varphi(\mathbf{x}, \mathbf{y}) = e^{-\alpha\mathbf{x}\cdot\mathbf{y}}$$

Setting

$$(4.4) \quad f_n(\mathbf{x}) = \frac{1}{n} \sum_{i=1}^n c_i \varphi(\mathbf{x}, \mathbf{y}_i) = \frac{1}{n} \sum_{i=1}^n c_i e^{-\alpha\mathbf{x}\cdot\mathbf{y}_i},$$

the GD flow in (2.1) can then be written explicitly as

$$(4.5) \quad \begin{cases} \dot{\mathbf{Y}}_i = C_i \nabla f(\mathbf{Y}_i) + \frac{\alpha}{n} \sum_{j=1}^n C_j C_j \mathbf{Y}_j e^{-\alpha\mathbf{Y}_i \cdot \mathbf{Y}_j} - \lambda_i \mathbf{Y}_i \\ \dot{C}_i = f(\mathbf{Y}_i) - \frac{1}{n} \sum_{j=1}^n C_j e^{-\alpha\mathbf{Y}_i \cdot \mathbf{Y}_j} \end{cases}$$

where $-\lambda_i \mathbf{Y}_i$ is a Lagrange multiplier term added to enforce $|\mathbf{Y}_i| = \sqrt{d}$ for all $i = 1, \dots, n$, $f(\mathbf{x})$ is given by (4.1) and $\nabla f(\mathbf{x})$ is given componentwise by

$$(4.6) \quad \frac{\partial f}{\partial x_p} = \frac{1}{d} \sum_{q,r=1}^d (a_{p,q,r} + a_{r,p,q} + a_{q,r,p}) x_q x_r,$$

As apparent from (4.5) the advantage of using radial basis function networks is that we can use $f(\mathbf{x})$ and the kernel $\varphi(\mathbf{x}, \mathbf{y})$ directly, and do not need to evaluate $F(\mathbf{y})$ and $K(\mathbf{y}, \mathbf{y}')$ (that is, we need no batch). In other words, the cost of running (4.5) scales like $(dn)^2$, instead of $P(Nn)^2$ in the case of a general network optimized by SGD with a batch of size P and $\mathbf{y} \in D \subset \mathbb{R}^N$. If we make P scale with n , like $P = Cn^{2\alpha}$ for some $C > 0$, as we need to do to obtain the scalings discussed in Sec. 3, the cost of SGD becomes $N^2 n^{2+2\alpha}$, which is quickly becomes much worse than $(dn)^2$ as n grows.

We tested the representation (4.4) in $d = 5$ using $n = 16, 32, 64, 128$, and 256 and setting $\alpha = 5/d = 1$. The training was done by running a time-discretized version of (4.5) with time step $\Delta t = 10^3$ for 2×10^5 steps: during the first 10^5 we added a bit of thermal noise to (4.5), which we then remove during the second half of the run. The representation (4.4) proves to be accurate

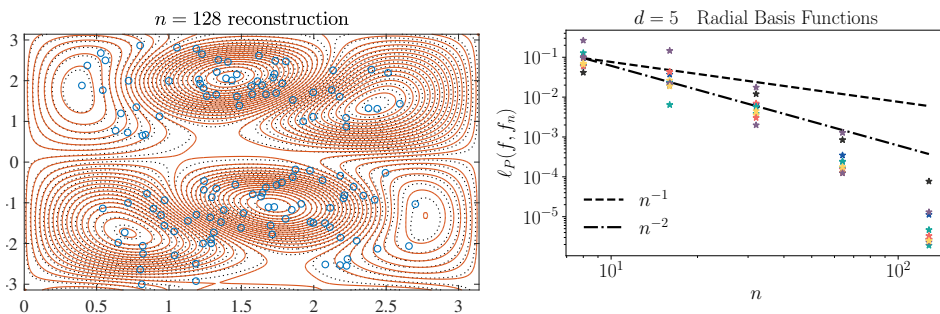


FIGURE 1. Left panel: Comparison between the level sets of the original function f in (4.1) (black dotted curves) and its approximation by the neural network in (4.4) with $n = 128$ and $d = 5$ in the slice defined by (4.7). Also shown are the projection in the slice of the particle position. Right panel: empirical loss in (4.8) vs n at the end of the calculation. The stars show the empirical loss for 10 independent realizations of the coefficients $a_{p,q,r}$ in (4.1), the full circles show their average value.

even at rather low value of n : for example, the right panel of Fig. 1 shows a contour plot of the original function f and its representation f_n with $n = 128$ through a slice of the sphere as

$$(4.7) \quad \mathbf{x}(\theta) = \sqrt{d} (\sin(\theta) \cos(\varphi), \sin(\theta) \sin(\varphi), \cos(\theta), 0, 0), \quad \theta \in [0, \pi], \quad \varphi \in [0, 2\pi).$$

The level sets of both functions are in good agreement. Also shown on this figure is the projection on the slice of the position of the 64 particles on the sphere. In this result, the parameters c_i took values that were rather uniformly distributed by about $-40d^2 = -10^3$ and $40d^2 = 10^3$. To test the accuracy of the representation, we used the following Monte Carlo estimate of the loss function

$$(4.8) \quad \ell_P(f, f_n(t)) = \frac{1}{2P} \sum_{p=1}^P |f(\mathbf{x}_p) - f_n(t, \mathbf{x}_p)|^2.$$

This empirical loss function was computed with a batch of 10^6 points \mathbf{x}_p uniformly distributed on the sphere. The value (4.8) calculated at the end of the calculation is shown as a function of n in the right panel of Fig. 1: the empty circles show (4.8) for 4 individual realizations of the coefficient $a_{p,q,r}$ in (4.1), the full circle shows the average of (4.8) over these 4 realizations. The blue line scale as n^{-1} , the red one as n^{-2} : as can be seen, the empirical loss decays with n faster than n^{-1} , which is as expected.

4.2. Learning with single layer networks with sigmoid nonlinearity. To further test our predictions and also assess the learnability of high dimensional functions, we used 3-spin models in $d = 10$ and 25 dimensions, which we approximated with a single-layer neural network with sigmoid nonlinearity parameterized by $\mathbf{y} = (\mathbf{a}, b) \in D = \mathbb{R}^{d+1}$, with $\mathbf{a} \in \mathbb{R}^d$, $b \in \mathbb{R}^d$, and

$$(4.9) \quad \varphi(\mathbf{x}, \mathbf{y}) = h(\mathbf{a} \cdot \mathbf{x} + b)$$

This gives

$$(4.10) \quad f_n(\mathbf{x}) = \frac{1}{n} \sum_{i=1}^n c_i h(\mathbf{a}_i \cdot \mathbf{x} + b_i)$$

where $h(z) = 1/(1 + e^{-z})$. Simple networks like these, as opposed to deep neural with many parameters, provide greater assurance that we have trained sufficiently to test the scaling.

We trained the model in (4.10) using SGD with an initial batch of $P = \lfloor n/5 \rfloor$ points uniformly sampled on the sphere for 2×10^6 time steps, resampling a new batch at every time step: this corresponds to choosing $\alpha = 1/2$ in the notation of Sec. 3. Towards the end of the trajectory,

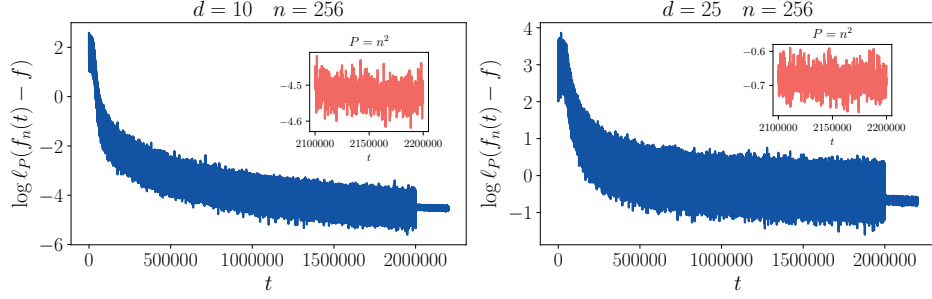


FIGURE 2. The log of the empirical loss in (4.8) as a function of training time by SGD for the sigmoid neural network in $d = 10$ (left panel) and $d = 25$ (right panel). At time $t = 2 \times 10^6$, the batch size is increased to initiate a quench. The insets show the log of the empirical loss as a function of time during the final 10^5 time steps of training.

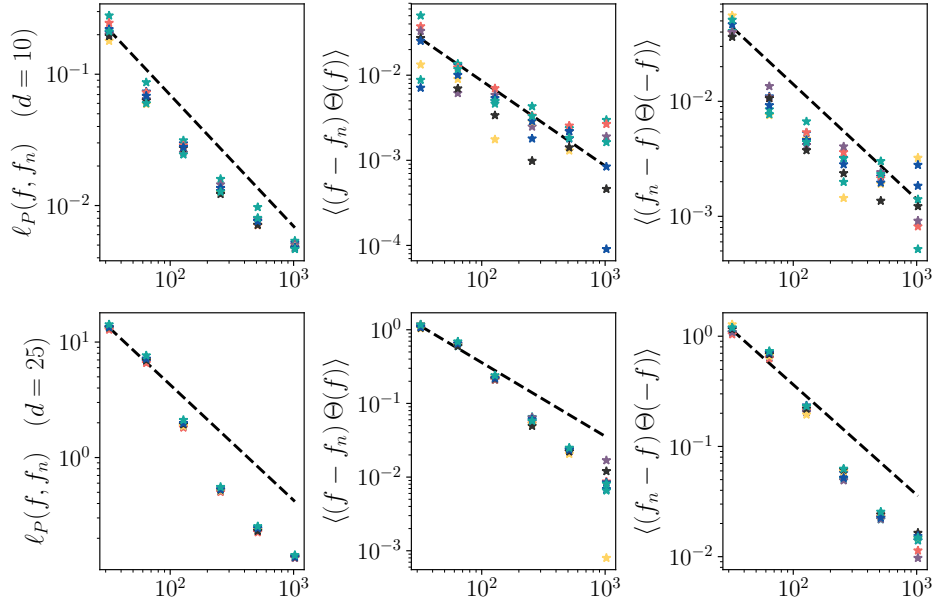


FIGURE 3. Error scaling for single layer neural network with sigmoid nonlinearities. Upper row: $d = 10$; lower row: $d = 25$. The first column shows the empirical loss in (4.8), the second column shows (4.11), and the third column shows (4.11) with $\Theta(f)$ replaced by $\Theta(-f)$. The stars show the results for 10 different realizations of the coefficients $a_{p,q,r}$ in (4.1): the dashed lines decay as n^{-1} , consistent with the predictions in (3.34) and (3.36).

we initiated a partial quench by increasing the batch size to $P = \lfloor (n/5)^2 \rfloor$ (i.e. $\alpha = 1$) which we run for an additional 2×10^5 time steps. Fig. 2 shows the empirical loss in (4.8) calculated over the batch as a function of training time during the optimization with $n = 256$ particles and $d = 10$ (left panel) and $d = 25$ (right panel). Note that the lack of intermediate plateaus in the loss during training is consistent with our conclusion that the dynamics effectively descends on a quadratic energy landscape (i.e. the loss function itself) at the level of the empirical distribution of the

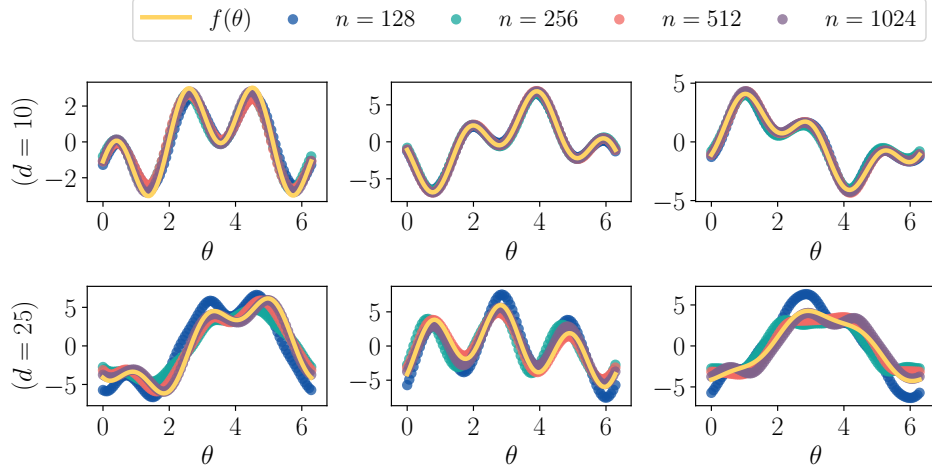


FIGURE 4. One dimensional slices through the $d = 10$ (upper row) and $d = 25$ (lower row) neural net representation f_n are shown below a yellow curve with the target function f . In $d = 10$, the function representations clearly capture the main features of the target function, with only small scale deviations. In $d = 25$ there is remarkably good signal when $n = 1024$ while the smaller neural network is less able to faithfully represent the target function.

particles. After the quench the empirical loss shows substantially smaller fluctuations as a function of time which helps to reduce the fluctuating error. The inset shows the final 10^5 time steps in which there is negligible downward drift, indicating convergence towards stationarity at this batch size.

In these higher dimensional examples, we tested the scaling with three different observables. First, we considered the empirical loss function in (4.8) which we computed over a batch of size $\hat{P} = 10^5$ larger than P . As shown in the two right panels Fig. 3, $\ell_{\hat{P}}(f, f_n(t))$ scales as n^{-1} , consistent with the estimate in (3.36) with $\alpha = 1$. We also tested the estimate in (3.34) using

$$(4.11) \quad \frac{1}{\hat{P}} \sum_{p=1}^{\hat{P}} \Theta(f(\mathbf{x}_p)) (f(\mathbf{x}_p) - f_n(t, \mathbf{x}_p)),$$

and similarly with $\Theta(-f(\mathbf{x}_p))$: here Θ denotes the Heaviside function. The result is shown in the four right panels in Fig. 3: (4.11) scales as n^{-1} , consistent with (3.34) and our choice of $\alpha = 1$.

To provide further confidence in the quality of the representations, we also made a visual comparison by plotting f and f_n along great circles of the sphere. We do so by picking $i \neq j$ in $\{1, \dots, d\}$ and setting $\mathbf{x} = \mathbf{x}(\theta) = (x_1(\theta), \dots, x_d(\theta))$ with

$$(4.12) \quad x_i(\theta) = \sqrt{d} \cos(\theta), \quad x_j(\theta) = \sqrt{d} \sin(\theta), \quad x_k(\theta) = 0 \quad \forall k \neq i, j.$$

In Fig. 4 we plot $f(\mathbf{x}(\theta))$ and $f_n(\mathbf{x}(\theta))$ along three great circles for $d = 10$ and $d = 25$. As can be seen, the agreement is quite good and confirms the quality of the final fit. A strong signal is present in $d = 25$ with $n = 1024$, a remarkable fact when considering that if we had only two grid points per dimension, the total number of points in the grid would be $2^{25} = 33,554,432$.

5. CONCLUDING REMARKS

Viewing parameters as particles with the loss function as interaction potential enables us to leverage a powerful theoretical apparatus developed in the context of large systems of interacting particles. Using these ideas, we can analyze the approximation quality and the trainability

of neural network representations of high-dimensional functions. Several insights emerge from our analysis based on this viewpoint. First, these tools show that the Universal Approximation Theorem follows from a Law of Large Numbers for the empirical distribution of the parameters / particles. Moreover, our results enrich the more abstract derivations of the Universal Approximation Theorem with a dynamical perspective. Specifically, we conclude that the empirical distribution effectively descends on the quadratic loss function landscape when the number n of parameters in the network is large. This confirms the empirical observation that neural networks are trainable despite the non-convexity of the loss function viewed from the individual particles perspective (as opposed to that of their empirical distribution). Secondly, we have derived a Central Limit Theorem for the empirical distribution of the particles, specifying the approximation error of neural network representation and showing that it is universal.

We derived these results first in the context of gradient descent dynamics of the particles / parameters; however, they also apply to stochastic gradient descent. The analysis indicates how the parameters in SGD should be chosen, in particular how the batch size should be scaled with n given the time step used in the scheme, which can be done towards the end of training.

Our numerical results confirm these predictions, as well as the capability of neural networks to represent high-dimensional function accurately with a relatively modest number of adjustable parameters. Needless to say, this feat opens the door to developments in scientific computing that we are only beginning to grasp. Such applications will benefit from better understanding how the specific architecture of the neural networks affects the approximation error and trainability, not in the general terms of their scaling with n that we analyzed here, but in the details of the constant involved.

REFERENCES

- [1] Yann LeCun, Yoshua Bengio, and Geoffrey Hinton. Deep learning. *Nature*, 521(7553):436–444, May 2015.
- [2] Jörg Behler and Michele Parrinello. Generalized Neural-Network Representation of High-Dimensional Potential-Energy Surfaces. *Phys. Rev. Lett.*, 98(14):583, April 2007.
- [3] Elia Schneider, Luke Dai, Robert Q Topper, Christof Drechsel-Grau, and Mark E Tuckerman. Stochastic Neural Network Approach for Learning High-Dimensional Free Energy Surfaces. *Phys. Rev. Lett.*, 119(15):150601, October 2017.
- [4] Yuehaw Khoo, Jianfeng Lu, and Lexing Ying. Solving for high dimensional committor functions using artificial neural networks. *arXiv:1802.10275*, February 2018.
- [5] Jens Berg and Kaj Nyström. A unified deep artificial neural network approach to partial differential equations in complex geometries. *arXiv:1711.06464*, November 2017.
- [6] W. E, J. Han, and A. Jentzen. Deep learning-based numerical methods for high-dimensional parabolic partial differential equations and backward stochastic differential equations. *arXiv:1706.04702*, June 2017.
- [7] C. Beck, W. E, and A. Jentzen. Machine learning approximation algorithms for high-dimensional fully nonlinear partial differential equations and second-order backward stochastic differential equations. *arXiv:1709.05963*, September 2017.
- [8] L. Zhang, J. Han, H. Wang, R. Car, and W. E. DeePCG: constructing coarse-grained models via deep neural networks. *arXiv:1802.08549*, February 2018.
- [9] G Cybenko. Approximation by superpositions of a sigmoidal function. *Math. Control Signal Systems*, 2(4):303–314, December 1989.
- [10] A R Barron. Universal approximation bounds for superpositions of a sigmoidal function. *IEEE Transactions on Information Theory*, 39(3):930–945, May 1993.
- [11] J Park and I W Sandberg. Universal Approximation Using Radial-Basis-Function Networks. *Neural Computation*, 3(2):246–257, June 1991.
- [12] Léon Bottou and Yann L. Cun. Large scale online learning. In S. Thrun, L. K. Saul, and B. Schölkopf, editors, *Advances in Neural Information Processing Systems 16*, pages 217–224. MIT Press, 2004.
- [13] Levent Sagun, V Ugur Guney, Gérard Ben Arous, and Yann LeCun. Explorations on high dimensional landscapes. *arXiv:1412.6615*, December 2014.
- [14] Anna Choromanska, Mikael Henaff, Michael Mathieu, Gérard Ben Arous, and Yann LeCun. The Loss Surfaces of Multilayer Networks. *arXiv:1412.0233*, November 2014.
- [15] M. Baity-Jesi, L. Sagun, M. Geiger, S. Spigler, G. Ben Arous, C. Cammarota, Y. LeCun, M. Wyart, and G. Biroli. Comparing Dynamics: Deep Neural Networks versus Glassy Systems. *arXiv:1803.06969*, March 2018.
- [16] S. Mei, A. Montanari, and P.-M. Nguyen. A Mean Field View of the Landscape of Two-Layers Neural Networks. *arXiv:1804.06561*, April 2018.

- [17] Claude Kipnis and Claudio Landim. *Scaling limits of interacting particle systems*, volume 320. Springer Science & Business Media, 2013.
- [18] Sylvia Serfaty. *Coulomb gases and Ginzburg-Landau vortices*. Zurich Lectures in Advanced Mathematics. European Mathematical Society Publishing House, 2015.
- [19] Thomas Leblé and Sylvia Serfaty. Large deviation principle for empirical fields of log and riesz gases. *Inventiones mathematicae*, 210(3):645–757, 2017.
- [20] Sylvia Serfaty. Systems of Points with Coulomb Interactions. *arXiv:1712.04095*, December 2017.
- [21] C W Groetsch. *The theory of Tikhonov regularization for Fredholm equations of the first kind*, volume 105 of *Research Notes in Mathematics*. Pitman (Advanced Publishing Program), Boston, MA, 1984.
- [22] David S Dean. Langevin equation for the density of a system of interacting Langevin processes. *J. Phys. A: Math. Gen.*, 29(24):L613–L617, January 1999.
- [23] Qianxiao Li, Cheng Tai, and Weinan E. Dynamics of stochastic gradient algorithms. *CoRR*, abs/1511.06251, 2015.
- [24] Wenqing Hu, Chris Junchi Li, Lei Li, and Jian-Guo Liu. On the diffusion approximation of nonconvex stochastic gradient descent. *arXiv:1705.07562*, May 2017.
- [25] Antonio Auffinger and Gérard Ben Arous. Complexity of random smooth functions on the high-dimensional sphere. *The Annals of Probability*, 41(6):4214–4247, November 2013.
- [26] Antonio Auffinger, Gérard Ben Arous, and Jiří Černý. Random Matrices and Complexity of Spin Glasses. *Comm. Pure Appl. Math.*, 66(2):165–201, 2012.

COURANT INSTITUTE OF MATHEMATICAL SCIENCES, NEW YORK UNIVERSITY, 251 MERCER STREET, NEW YORK, NY 10012

E-mail address: rotskoff@cims.nyu.edu, eve2@cims.nyu.edu